

Department of Advanced Materials Science,

Graduate School of Frontier Sciences,

The University of Tokyo

2022

Master's Thesis

Synthesis and characterization of non-aromatic heat-resistant polymers

(非芳香族系耐熱性ポリマーの合成と物性評価)

Submitted July 19, 2022

Supervisor: Kazuaki Kato

47-206115: Wenhao Zhang (張文昊)

CONTENTS

CHAPTER 1. GENERAL INTRODUCTION	1
1.1 Heat-resistant polymers.....	1
1.2 Polymethylene.....	3
1.3 Aim and scope in this thesis	7
CHAPTER 2. SYNTHESSES OF POLYMETHYLENE	8
2.1 Introduction.....	8
2.2 Synthesis of polymethylene salts by carbene polymerization.....	9
2.2.1 Polymerization of poly(ethoxycarbonylmethylene).....	9
2.2.2 Hydrolysis of poly(ethoxycarbonylmethylene).....	10
2.3 Synthesis of polymethylene salts by radical polymerization.....	11
2.3.1 Synthesis of di-tert-butyl fumarate.....	11
2.3.2 Free radical polymerization of poly (di-tert-butyl fumarate)	12
2.3.3 Synthesis of poly(fumaric acid) by pyrolysis.....	13
2.3.4 Synthesis of poly(di-metal fumarate).....	13
2.4 Synthesis of cross-linked polymethylene	15
2.4.1 Cross-linked heat-resistant polymers	15
2.4.2 Cross-linked polymer gels.....	16
CHAPTER 3. CHARACTERIZATIONS OF POLYMETHYLENE	18
3.1 Nuclear Magnetic Resonance Spectroscopy (NMR).....	18
3.1.1 ¹ H NMR spectroscopy.....	18
3.1.2 ¹³ C NMR spectroscopy.....	22
3.1.3 Heteronuclear Multiple-Quantum Correlation	24
3.2 Gel Permeation Chromatography (GPC).....	25
3.3 Fourier Transform Infrared Spectroscopy (FT-IR).....	27
3.4 Scanning Electron Microscope- Energy Dispersive X-ray Spectroscopy (SEM-EDS).....	28
3.5 Optical Microscope	30
3.6 X-ray Diffraction (XRD).....	32
CHAPTER 4. THERMAL AND OPTICAL PROPERTIES OF POLYMETHYLENE	33
4.1 Thermal analyses.....	33
4.1.1 Thermal gravimetric(TG) analysis	33
4.1.2 Differential scanning calorimetry (DSC)	37
4.2 Transmittance measurements	38
4.2.1 UV-vis spectroscopy.....	38
4.2.2 Total transmittance and Haze	39
CHAPTER 5. SUMMARY AND PROSPECTS	40

ACKNOWLEDGMENTS	41
REFERENCES	42

CHAPTER 1. GENERAL INTRODUCTION

1.1 Heat-resistant polymers

Heat-resistant polymer materials have been used in a wide range of industrial fields, from aerospace to construction, microelectronics, etc. There are many criteria for evaluating heat-resistance of polymers. One of the representative definitions is the ability of a polymer to maintain their physical and mechanical properties at 250°C for long-term periods, at 500°C for medium-term periods and up to 1000°C for a few seconds¹.

There are several thermal criteria are considered for estimating the heat-resistance in various application. For instance, melting temperature, softening point, thermal decomposition temperature, and glass transition temperature. They can be summarized in two aspects: 1) thermal softening behavior of polymer main chain. 2) thermal stability (oxidative stability and non-oxidative stability). And the most representative thermal properties are glass transition temperature (T_g) and thermal decomposition temperature (T_d). T_g is the temperature of glass transition which refers to a gradual and reversible transition in amorphous materials (or in amorphous regions within semicrystalline materials) from a hard and relatively brittle "glassy" state into a viscous or rubbery state as the temperature is increased. T_d is the temperature at which the chemical decomposition of a substance occurs and is usually referred to in thermal gravimetric analysis, where temperature at which a weight loss of 5% occurs. Due to T_d always higher than T_g , T_g is generally more important for evaluating the heat-resistance of materials.

The development of heat-resistant polymers began in the late 1950s and early 1960s with the aim of providing polymers with sufficient heat-resistance to meet the needs of the aerospace and electronics industries. In the aerospace field, skin temperatures are around 110°C for more than 2 hours during the main part of the flight. Therefore, the materials of construction must be capable to withstand such temperatures for the flight life of the aircraft². In the electronic field, for instance, thin-film transistor-driven active matrix liquid crystal display devices (TFT-LCDs) or active matrix organic light-emitting display devices (AMOLEDs), the processing temperature on the flexible plastic substrates might be higher than 300°C. Most of polymer optical films would not maintain their optical and mechanical properties at such high processing temperatures. Hence, transparent, colorless heat-resistant polymers have attracted increasing interest over the last few decades³.

The design of new molecules to meet the needs based on the structure of existing materials is a generally feasible approach. There are two ways of designing materials that are both resistant to high temperatures and have good light transmittance: 1) enhancing transmittance of heat-resistant materials. 2) improving the heat-resistance of materials with good transmittance. Common plastic with their range of T_g is shown in Figure 1. The plastic bottle, polyethylene terephthalate (PET), and the acrylic glass, polymethyl methacrylate (PMMA), whose T_g is around 70°C. The polycarbonate (PC) is around 120°C. Polyimide (PI), on the other hand, is the most representative heat-resistant polymer, with a T_g of even more than 300°C. However, as its color and heat-resistance are derived from the aromatic structure, the desire to improve the transmittance also means

losing the heat-resistance. Therefore, it is more feasible to improve the heat-resistance than to improve its light transmittance.

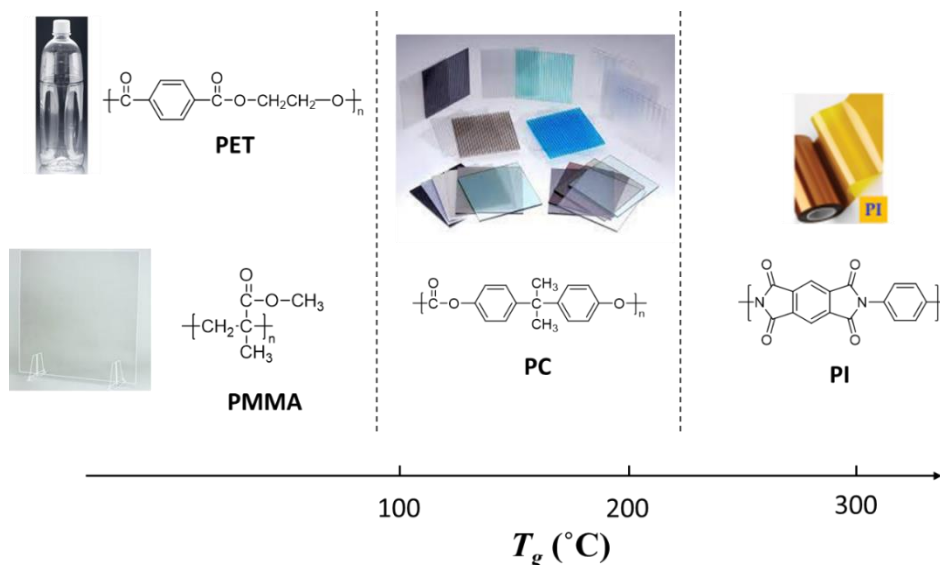


Figure 1. Common plastic with their range of T_g

There are many methods to improve the heat-resistance of polymers, the most significant of which are: cross-linking macromolecular chains, increasing the crystallinity of the polymer, increasing the rigidity of polymer main chain, removing weak bonds such as aliphatic, cycloaliphatic, NH etc. from the structure, adding strong bonds to the structure such as aromatic, ionic bonds etc., and adding heat-resistant micro or nano scale fillers into the polymer.

The heat-resistance of polymers is influenced by two main aspects: physical and chemical. From a physical point of view, there are several factors that weaken or enhance the heat-resistance of the polymer, such as the rigidity of the polymer chains. The glass transition is a relaxation phenomenon in terms of molecular motion, which is associated with micro-Brownian motion, that is the rotational motion of the main chain bonds. The more rigid the polymer chain is, the more difficult the rotation of the bonds is and the higher T_g polymers have. In addition, the increase of molecular weight and cross-linking reactions lead to an improvement of heat-resistance of the polymers due to the interactions of polymer chains increased. Crystallinity also contributes to thermal stability, which works by physically cross-linking, thus increasing the rigidity of the chains.

From a chemical point of view, the strength of the primary bonds in the macromolecular chain is an important parameter affecting the thermal resistance of a polymer. In short, the stronger the primary bond, the more thermally stable the polymers are. The thermal-mechanical properties are deteriorated by the reduction in molecular weight due to chemical bond breaking. Aromatic rings are very stable covalent bonds because of the resonance stability of their delocalized electrons. Therefore, most of the research on heat-resistant polymer materials has been carried out on aromatic structures.

Besides, introduction of other chemical bonds such as ionic bonds will also improve the T_g , for instance, poly(acrylic acid) neutralizes with sodium hydroxide to get poly(sodium acrylate) and the T_g rose from 106°C to 230°C⁴.

1.2 Polymethylene

To synthesize a new transparent heat-resistant polymer, a rigid molecular structure that does not contain an aromatic structure is the best choice according to the above discussion of methods to improve the heat-resistance of polymers. Among the various polymers, polymethylene attracted my attention. It is well known that polyethylene oxide (PEO) which has oxyethylene repeating unit is widely used in pharmaceutical, chemical and biological fields, and the melting point is around 68°C⁵. And the melting point of polyformaldehyde with oxymethylene repeating unit is around 198 °C⁶. The melting point is increased significantly because polyformaldehyde has a high degree of crystallinity and is influenced by the side chain substituents.

Substituted polymethylene is the polymer with substituents on all their main chain carbon atoms, or we can call them poly(1,2-substituted ethylene). These polymers are expected to have unique properties because their main chain structure is rigid, and different from mono-substituted vinyl and 1,1-disubstituted vinylidene polymers, which have a methylene spacer in the main chain⁷.

Substituted polymethylene are generally considered not to homopolymerize in common radical initiator because of the strong steric hindrance of propagation step. However, a series of di-alkyl fumarates with bulky alkyl ester groups have been reported to carry out high molecular weight polymerization in the presence of free radical initiators⁸⁻¹⁶. And there is another synthetic strategy for substituted polymethylene, the polymerization of diazoacetates¹⁶⁻²⁸.

As for synthesis of substitute polymethylene by free radical polymerization, the homopolymerization of di-alkyl fumarates is very delicate. It is sensitive to the structure of ester groups but also to the polymerization conditions such as the presence of solvent and traces of oxygen or the purity of initiators and monomers. For those polymers with different substitutes which are successfully synthesized, I summarized their structure in figure 2 and their thermal properties in Table 1. Polymers are polymerized directly from the monomers except poly(fumaric acid). Typical 1,2-substituted ethylenic monomers such as maleic acid and fumaric acid have been known to be not homopolymerized, not only does the steric hindrance make it difficult for propagation, but also because the electron withdrawing group make the radical unstable. It has been shown that the t-butyl group promote polymerization reactivity not only the acceleration of propagation step despite the strong steric repulsion, but also by the deceleration of the termination step³⁰. It was shown the result from extremely slow bimolecular termination of the substituted polymethylene radicals with a rigid chain structure, thus overcompensating the slowing down of the propagation step. Those polymers are considered to have a rigid backbone structure, and their T_g is generally not observable with DSC. Among of them, poly[di(1-adamantyl) fumarate] shows best thermal stability with the highest T_d ³¹.

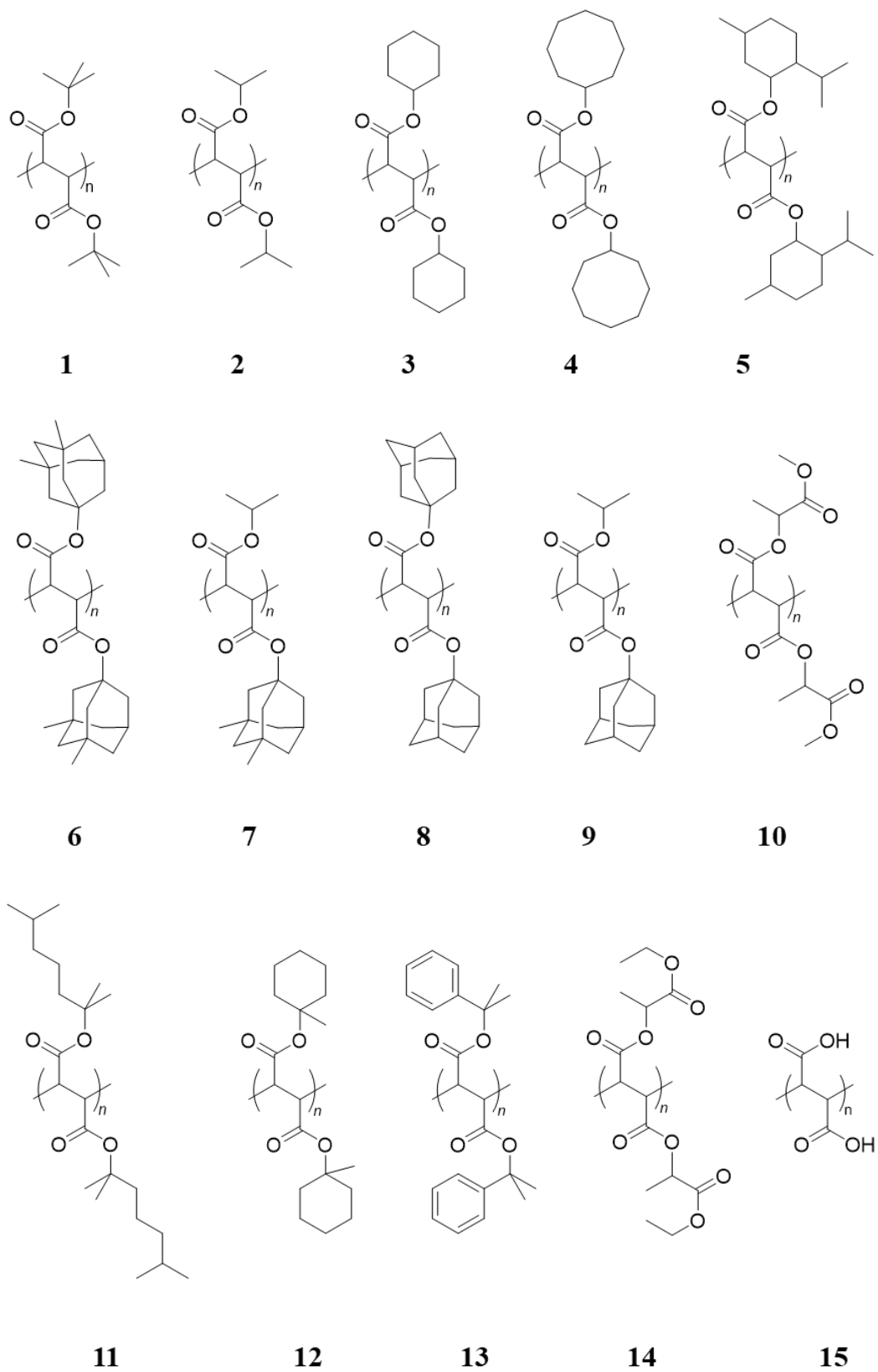


Figure 2. Structural formula of poly(fumarates)

Table 1. Thermal properties of poly(fumarate)

No.	name	$T_g / ^\circ\text{C}$	$T_d / ^\circ\text{C}$
1	poly(di-tert-butyl fumarate)	-	170 ^a (195-200) ^b
2	poly(di-isopropyl fumarate)	74	223(start) 300(maximum degradation rate)
3	poly(di-cyclohexyl fumarate)	-	290-295
4	poly(di-cyclooctyl fumarate)	-	245-250
5	poly(di-menthyl fumarate)	-	260-265
6	poly[bis(3,5-dimethyl-1-adamantyl) fumarate]	-	329
7	poly(3,5-dimethyl-1-adamantyl isopropyl fumarate)	-	286
8	poly[di(1-adamantyl) fumarate]	-	384
9	poly(1-adamantyl isopropyl fumarate)	-	288
10	poly(di-methyl lactate fumarate)	66	265-275
11	poly[di(2,6-dimethyl hept-2-yl) fumarate]	-3	200-205 (first step) 250-255 (second step)
12	poly[di(1-methyl cyclohexyl)fumarate]	-	210-215 (first step) 255-260 (second step)
13	poly[di(1,1-dimethyl benzyl)fumarate]	-	120-130 (first step) 255-260 (second step)
14	poly[di(2,2-dimethyl ethyl propionate) fumarate]	-	255-260 (first step) 365-370 (second step)
15	poly(fumaric acid)	-	300

^a Temperature of pyrolysis in this work

^b Temperature of pyrolysis from the reference⁸

C1 polymerization which is the methods for preparing polymers from “*one carbon unit*” is another strategy for synthesis of poly(substituted methylene)²⁹. One of the representative examples of C1 polymerization is the polymerization of diazoalkanes. For instance, BF₃-initiated polymerization of diazomethane yields high molecular weight polymethylene with a structure essentially identical to that of linear polyethylene³². Several research groups have at least partially achieved important objectives, such as the synthesis of high M_n polymers and stereospecific polymerization initiated by rhodium-based initiator or controlled polymerization related to M_n and PDI with palladium-based initiator, and the synthesis of functional polymers with unique photophysical properties¹⁹ or ability of self-assembly³³.

1.3 Aim and scope in this thesis

The primary motivation for this study is synthesis and characterization of transparent heat-resistant polymers. As described above, since the current excellent heat-resistant polymer materials usually have darker color with aromatic ring structure, transparent and colorless heat-resistant polymers have attracted increasing interest. And substituted polymethylene shows potential to achieve outstanding heat-resistance with non-aromatic structure. Therefore, in this thesis, the concept of polymer design starting from poly(acrylic acid) (PAA) to poly(fumaric acid) (PFA) by reducing the methylene spacers in the repeating units. Based on this, there are two ideas to improve the thermal properties:

1. Neutralizing with different metal hydroxides to obtain poly(carboxylate).
2. Cross-linking with diamine or diol to increase the inter-chain interactions.

And these polymers will be evaluated in two main aspects:

1. Thermal properties: T_d and T_g .
2. Optical properties: *Transmittance* and *Haze* of UV and visible light

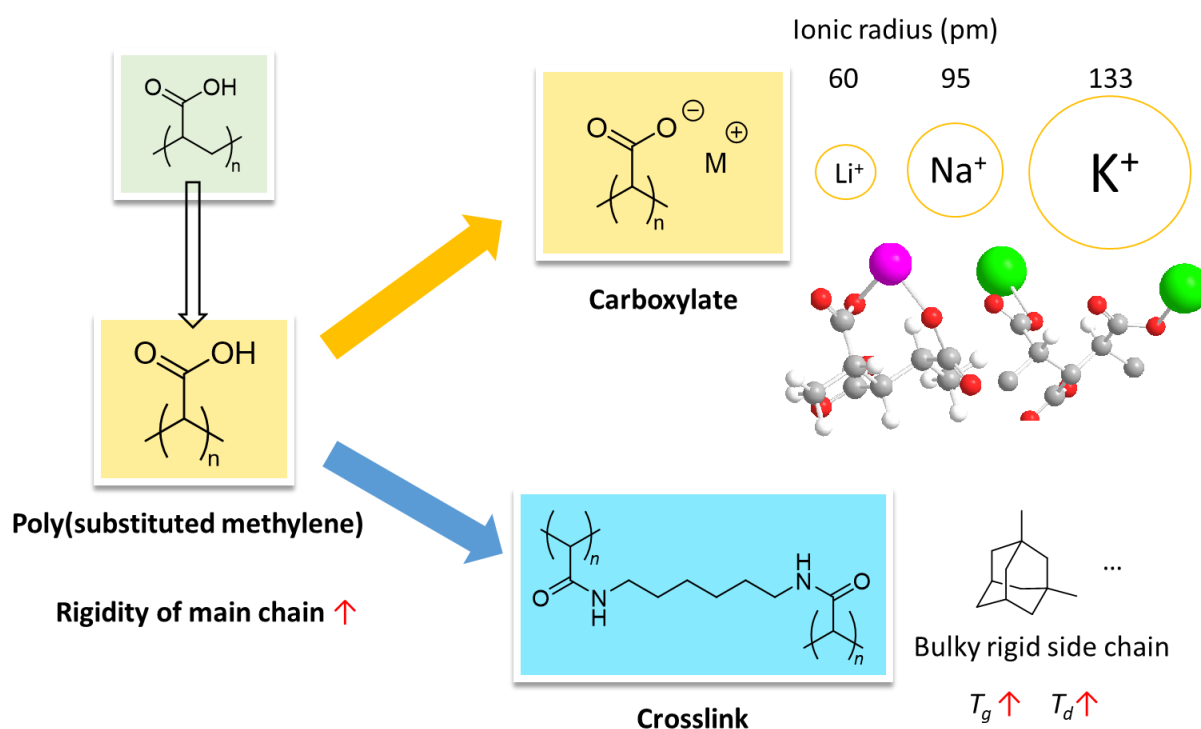


Figure 3. Two strategies for improving thermal properties.

Based on these objectives, this thesis comprises 5 chapters on synthesis and characterization of target non-aromatic heat-resistant polymers. Chapter 1 introduces the challenge of heat-resistant polymer materials and the potential of substituted polymethylene for excellent heat-resistance. Chapter 2 demonstrates details about synthesis of different polymers such as yields and molecular weight. In Chapter 3 and 4, structure characterization and evaluation of thermal and optical properties are presented. Finally, major findings and further prospects of this study are highlighted in Chapter 5.

CHAPTER 2. SYNTHESIS OF POLYMETHYLENE

2.1 Introduction

To synthesize one of the target polymers, the salts of poly(fumaric acid) (PFA), two retrosynthetic strategies have been attempted as shown in Figure 4. Both these methods are polymerized into the substituted polymethylene with ester group firstly. Then the polymer of carboxylate was produced by hydrolysis from ester directly or by neutralization with PFA. As for the C1 polymerization, tert-butyl diazoacetate cannot be homo-polymerized because of the strong steric hindrance²⁶ and ethyl diazoacetate is relatively the most stable diazoacetate monomers. However, as mentioned above, the free radical polymerization of di-tert-butyl fumarate has the highest reactivity among di-alkyl fumarate monomer. Thus, the feasible synthesis routes are hydrolysis of poly(ethoxycarbonylmethylene) which is polymerized from ethyl diazoacetate by transition metal-initiator and neutralization with PFA which is polymerized from poly(di-tert-butyl fumarate) (PDtBF).

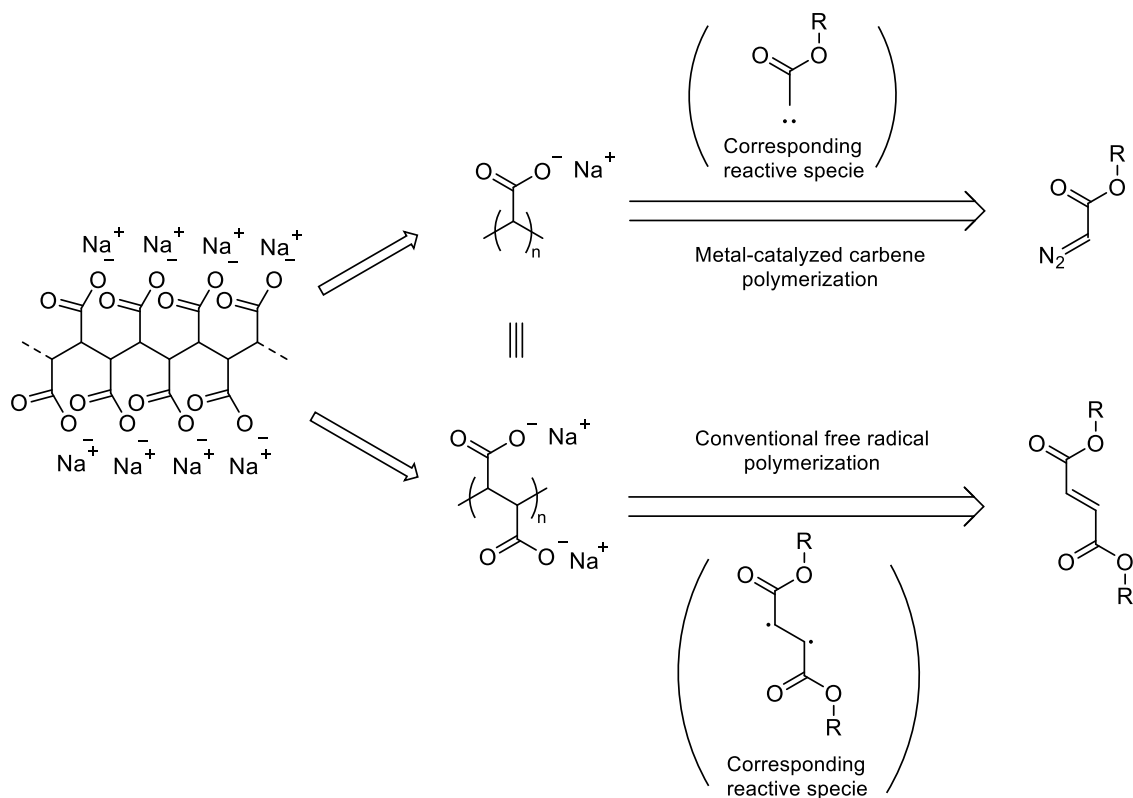


Figure 3. Retrosynthetic schemes of poly(carboxylate) with transition metal-initiated carbene polymerization of diazoacetate and radical polymerization of di-alkyl fumarate

To synthesize the crosslinked polymer, esterification from acyl chloride with diol and amidation with diamine are attempted. Cross-linking could not only improve thermal properties, but also expands other properties by synthesizing gels. For instance, sodium polyacrylate is well known as a hydrogel, and polymers in this thesis also have various hydrophilic groups in the structure.

2.2 Synthesis of polymethylene salts by carbene polymerization

2.2.1 Polymerization of poly(ethoxycarbonylmethylene)

To a solution of (π -allyl) palladium chloride dimer (0.25g, 0.68mmol) in 10mL dichloromethane (DCM), added silver acetate (0.24g, 2 eq.). The bright yellow solution was stirred for 15 minutes, and off-white precipitate of AgCl was filtered off using a PTFE filter. Solvent was evaporated and bright yellow solid was dried under a high vacuum. 0.24g pure (π -allyl) palladium acetate dimer was obtained in 85% yield.

To the stirring solution of ethyl diazoacetate (EDA) monomer (15% in toluene, 1.5mL, 200 eq.) under nitrogen atmosphere at -10°C was added a solution of a (π -allyl)palladium acetate dimer (3.6mg, 1 eq.) in DCM (12 mL). After reacting for 10 hours, the dark yellow solution was quenched by HCl (aq.) and washed by MeOH. The polymer was extracted by CHCl_3 . The organic phase was washed with HCl aqueous solution once again, filter by celite and dried with MgSO_4 . After evaporation of solvent, the residue was obtained in 86% yield.

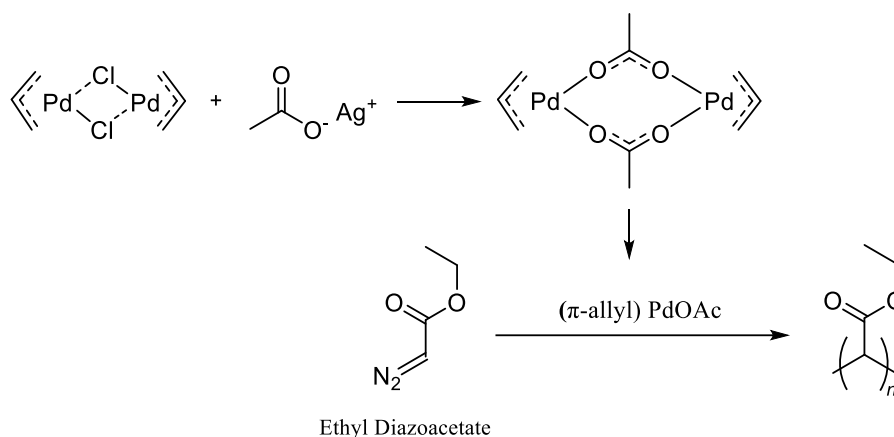


Figure 4. Synthesis of (π -allyl) palladium acetate dimer and poly(ethoxycarbonylmethylene)

2.2.2 Hydrolysis of poly(ethoxycarbonylmethylene)

To the solution of poly(ethoxycarbonylmethylene) in 1,4-dioxane was mixed with NaOH aqueous solution in PTFE coating pressure reactor. To make the reaction faster and increase conversion, the ratio of water and 1,4-dioxane was adjusted to 2:1, so that the solution tended to be homogeneous. After reacting at 180°C for 24 hours, solid precipitate and solution were obtained. It should be noted that glass flasks cannot be used for this hydrolysis, because at the reaction temperature, the reaction between alkali and glass is relatively rapid, and silica will precipitate out together after adding acid. The solution was quenched by HCl (aq.), and organic compounds were extracted by ethyl acetate. The solid was washed by water and dried under vacuum. The yield that was calculated by weight was 64%.

The compounds from solution were characterized by ^1H (400 MHz) NMR, however, there was no peak of the reactant polymer in spectrum. The solid didn't dissolve in any solvent, so that I analyzed the elements by FT-IR and SEM-EDS .

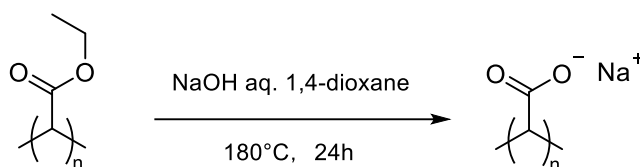


Figure 5. Hydrolysis of poly(ethoxycarbonylmethylene)

2.3 Synthesis of polymethylene salts by radical polymerization

2.3.1 Synthesis of di-tert-butyl fumarate

To a solution of tert-butyl alcohol (16.8g, 21.6mL, 0.22mol) in THF (60mL) cooled at -78°C by ethyl acetate (EtOAc) and liquid nitrogen with stirring under nitrogen atmosphere, n-BuLi (141mL, 1.6M in hexane) was added dropwisely. After mixing the solution for 2 hours at the same temperature, fumaryl chloride (16.8g, 12mL, 0.11mol) was added slowly. Then the cold bath was removed, and the mixture was stirred for overnight. The resulting solution was washed with a saturated NH_4Cl aqueous solution and EtOAc, and the organic phase was further washed with a saturated NaHCO_3 aqueous solution and saturated NaCl aqueous solution. The organic phase was dried with MgSO_4 , and the solvent was evaporated. The residue was purified by column chromatography on silica gel using hexane/EtOAc 95/5 as eluent. 21.17g white solid was obtained in 82% yield.

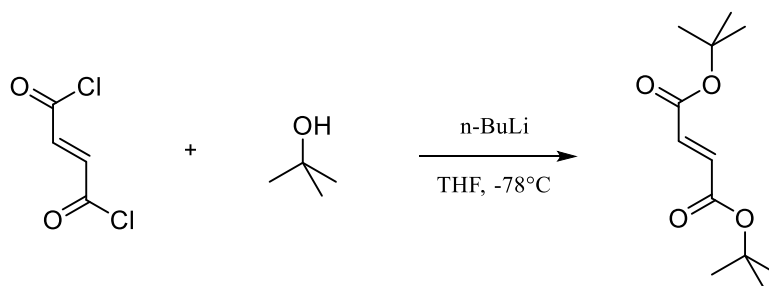


Figure 6. Synthesis of di-tert-butyl fumarate with tert-butyl alcohol

Another synthetic method which is usually used in research of poly(fumarate) has been attempted. However, compared with the above method, there are more side reactions, more difficult separations, and lower yield. The scheme is dissolving potassium tert-butoxide (22g, 0.196mol, 2.5eq.) in THF (75mL) cooled at -78°C by EtOAc and liquid nitrogen with stirring under nitrogen atmosphere, a solution of fumaryl chloride (12g, 0.078mol, 1.0eq.) in THF (75mL) was added slowly. After addition, the cold bath was removed, and the mixture was stirred for overnight. The purification was the same as above. Finally, 5g product was obtained in 30% yield.

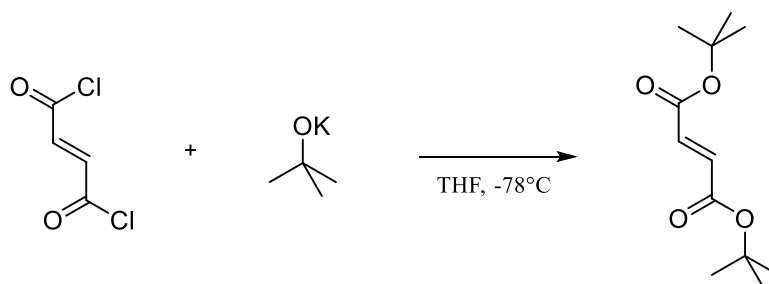


Figure 7. Synthesis of di-tert-butyl fumarate with potassium tert-butoxide

2.3.2 Free radical polymerization of poly (di-tert-butyl fumarate)

A mixture of di-tert-butyl fumarate (DtBF) and initiator in a glass tube was stirred at 75 °C under nitrogen for 16 h. The resulting mixture was diluted with THF and poured into a vigorously stirred methanol. The precipitate was collected by centrifuge and dried to obtain poly(di-tert-butyl fumarate). The polymer yield was determined based on the weight of precipitation. The polymerization was also carried out with 2,2'-Azodiisobutyronitrile (AIBN) and dimethyl azobis(isobutyrate) (MAIB) two kinds of initiator, different molar ratio of monomer/initiator, and different solvent conditions. The yield and molecular weight data are summarized in Table 2.

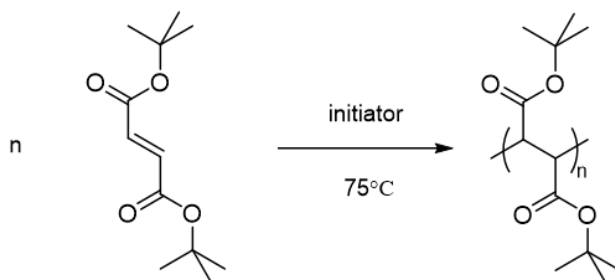


Figure 8. Free radical polymerization of poly (di-tert-butyl fumarate)

Table 2. Free-radical polymerization of DtBF in the presence of a radical initiator either in toluene or in bulk

DtBF(g)	Initiator	Solvent	Temp. (°C)	Time (h)	Yield	$M_n^c \times 10^{-4}$	M_w/M_n^c
0.3	2 mol% ^a	Toluene	70	16	- ^d	- ^d	- ^d
0.3	2 mol% ^a	none	75	16	77.8%	1.62	1.70
0.3	2 mol% ^b	Toluene	70	16	38.2%	0.30	1.75
0.3	2 mol% ^b	none	75	16	70.0%	0.97	2.34
1.5	2 mol% ^b	none	75	16	82.1%	1.12	2.69
2.5	2 mol% ^b	none	75	16	78.0%	3.04	3.99
3.0	2 mol% ^b	none	75	16	77.8%	3.86	3.33
10.0	2 mol% ^b	none	75	16	78.2%	10.8	1.81
0.4	1 mol% ^b	none	75	16	60.0%	4.18	3.70
0.2	0.2 mol% ^b	none	75	48	66.2%	5.49	3.25
0.2	0.04 mol% ^b	none	75	72	- ^d	13.8	1.71
0.2	0.008mol% ^b	none	75	72	- ^d	- ^d	- ^d
0.3	4 mol% ^b	Toluene	70	48	35.3%	0.43	1.81
0.3	6 mol% ^b	Toluene	70	48	65.0%	0.11	2.30

^a Polymerized by AIBN

^b Polymerized by MAIB

^c Analyzed by GPC and calibrated with PMMA standard

^d Not determined

2.3.3 Synthesis of poly(fumaric acid) by pyrolysis

Powder-like poly(di-tert-butyl fumarate) in glass sample bottle or flask was pyrolyzed in vacuum heater. The results for different experimental conditions are shown in Table 3. Yield was calculated by weight. The color of powder changed from white to yellow. PFA also showed different solubility before and after purification. Although the quantitative analysis was not done on the number of carboxyl group per repeating unit in the PFA sample, its chemical composition was characterized by the NMR spectrum, which has almost no peak of the t-butyl ester group. PFA also characterized by FT-IR spectrum, the details will be demonstrated in 3.3. The reasons for yields below 100% will be explained in Chapter 3.

Table 3. Pyrolysis of poly(di-tert-butyl fumarate)

PDtBF (g)	Temp. (°C)	Time (h)	Yield
1.5	150	16	92%
1.3	160	10	82%
2.0	170	2.5	85%
1.5	180	2	85%

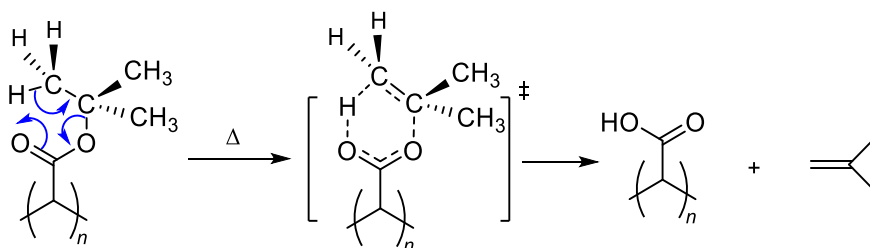


Figure 9. Pyrolysis mechanism of poly(di-tert-butyl fumarate)

2.3.4 Synthesis of poly(di-metal fumarate)

Monovalent ions: Li^+ , Na^+ , K^+ A solution of poly(fumaric acid) (PFA) in deionized water was added aqueous solution of metal hydroxide in different equivalent and stirred at room temperature for 24 hours. Polymers in solution would be purified by reprecipitation in methanol and collect by centrifuge, and the polymers precipitated from solution would be purified by washing with water and filtration.

It is worth noting that these three types of salts have different solubility in water and different abilities of forming film. During the dropwise addition of the alkaline solution, precipitates can be observed without stirring, and they can be dissolved again by shaking the sample bottle. If an excess of alkaline solution is added, the precipitates of sodium and lithium salts are no longer dissolved, and there is no precipitate generated from the salt of potassium. The precipitated lithium salt of PFA is soluble in neutral deionized water while the sodium salt is not. In addition, the solubility of PFA-Na is also related to the concentration of the solution used for neutralization. I tried using various concentrations for neutralization, and if the concentration of PFA-Na after neutralization is less than 5 mg/mL, no significant precipitation can be observed. At concentrations of 5 mg/mL, the insoluble precipitate was formed before complete neutralization.

Films of poly(di-metal fumarate) were prepared from aqueous solution of polymers, and the picture is shown in Figure 10. PFA-Li cannot form films with regular shapes. And PFA-Na does not form a film even when dried from a solution without insoluble precipitation, but leaves a powdered salt. It is important to note that the powder precipitated by drying is no longer soluble in water. Precipitation in polymer solutions can be considered to occur through three processes: 1) approach of a cation to an anion by electrostatic attraction, 2) elimination of solvated molecules from ions, and 3) formation of ionic binding between oppositely charged ions³⁴. The reason for the difference for polymers may be the crystallization of its structure or the molecular packing due to different ionic radius. I tried to verify my idea by microscopy and X-ray diffraction.

Divalent metal ions: Mg^{2+} , Zn^{2+} , Cu^{2+}

Poly(magnesium fumarate): A solution of poly(fumaric acid) in deionized water was added a solution of magnesium methoxide which synthesized from magnesium and methanol, stirred at room temperature until magnesium disappeared. White solid precipitated out immediately, and isolated by filtration. Yield calculated by dry weight was 228%

Poly(zinc fumarate) and poly(copper fumarate): A solution of poly(fumaric acid) in deionized water was added a solution of zinc/copper acetate in deionized water and stirred at room temperature. White (zinc)/blue (copper) solid also precipitated out immediately, and isolated by filtration. Yield calculated by dry weight was Zinc 162%, copper 110%.

Since divalent ions can easily form intermolecular crosslinks, low product solubility is expected. The reason for the high yield may be that some small molecules, such as water or the base, were trapped in the network structure, so that it is difficult to purify and dry.

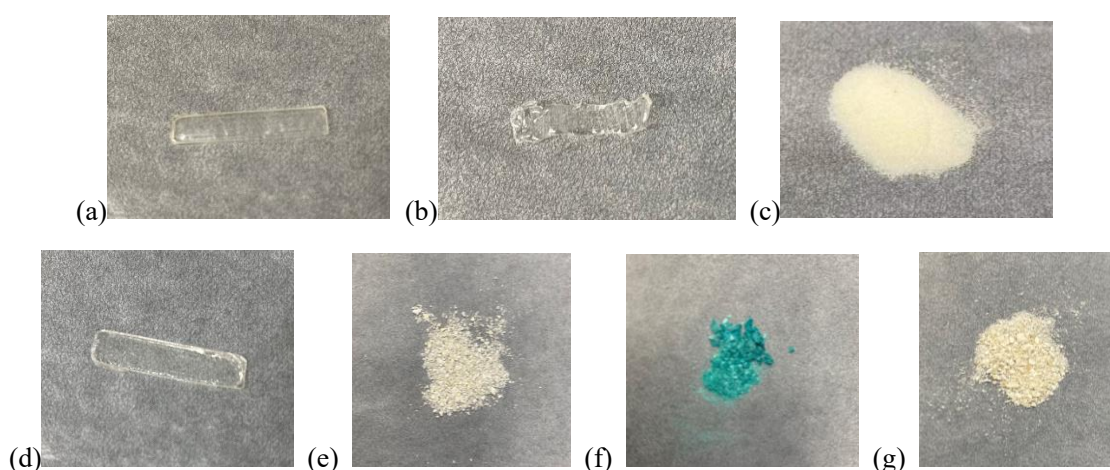


Figure 10. Pictures of sample (a) PFA film. (b) PFA-Li . (c) PFA-Na . (d) PFA-K film. (e) PFA-Mg. (f) PFA-Cu. (g) PFA-Zn.

2.4 Synthesis of cross-linked polymethylene

2.4.1 Cross-linked heat-resistant polymers

Cross-linked poly(fumaramide): To a solution of poly(fumaric acid) in dimethyl formamide(DMF) dried by molecular sieve mixed with solution of carbonyl diimidazole (CDI, 1.5 eq.) in DMF as the condensation agent for 1 hour. When the color of solution turned to brownish yellow, added hexamethylenediamine (HMDA, 0.6 eq.) or 1,3-adamantane diamine (ADA, 0.6 eq.) in DMF and stirred with a spatula until polymer precipitate at room temperature. The precipitates were washed with DMF and aqueous HCl then dried under vacuum. Yields calculated by weight were 11% (ADA) and 43% (HMDA)

Cross-linked poly(fumarate) : To a solution of poly(fumaric acid) in acetonitrile dried by molecular sieve, added SOCl_2 (5 eq.) dropwisely at 25°C for 4 hours. The color of the solution turned black and after evaporating solvent and thionyl chloride, a black solid which should be poly(fumaryl chloride) remained. To a solution of poly(fumaryl chloride) in acetonitrile added cyclohexanedimethanol (CHDM) at 40°C for 12 hours. A rubbery solid precipitated and washed with methanol. Addition of 1,3-adamantanediol in the same condition did not produce any precipitation, so the crosslinking by 1,3-adamantanediol was not successful.

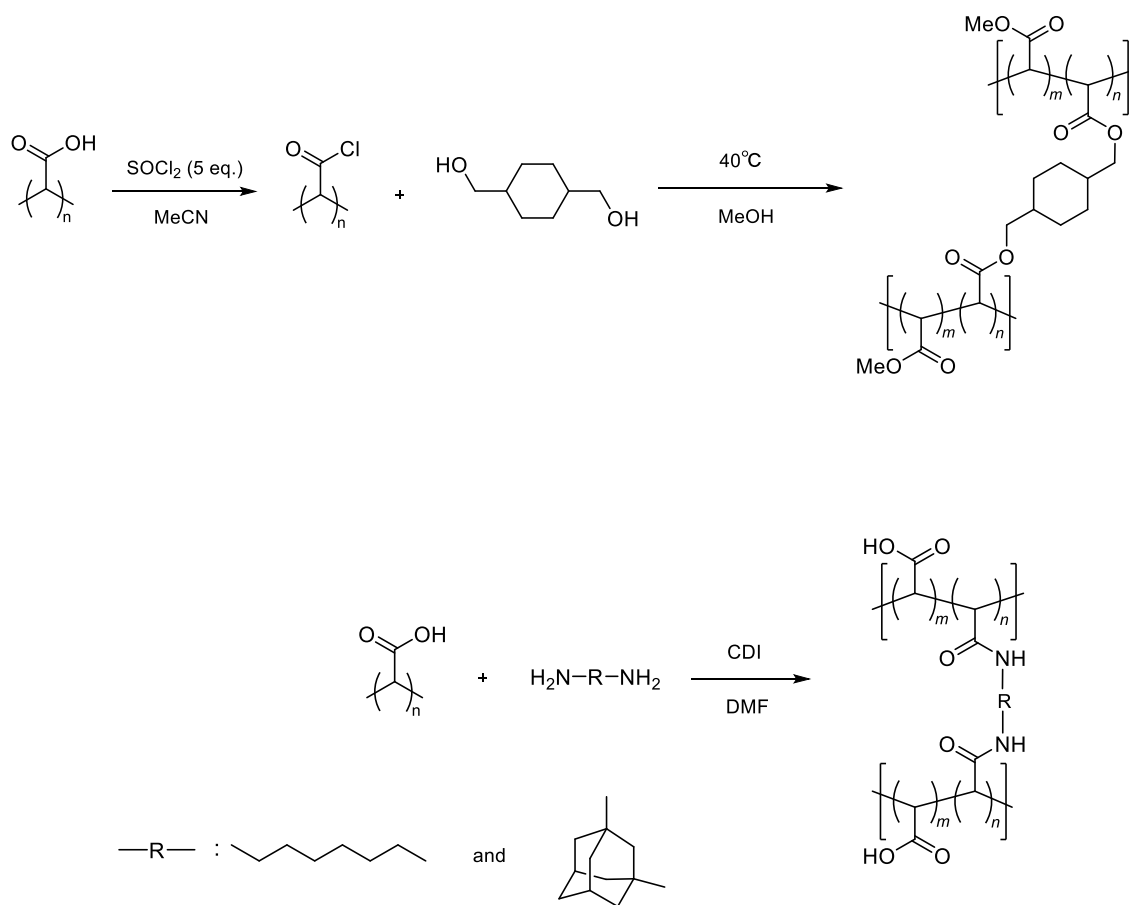
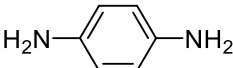
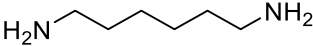
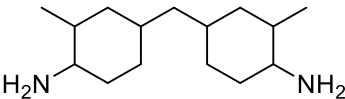
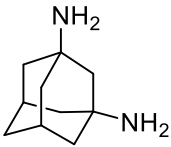
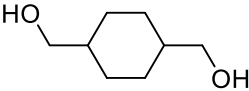
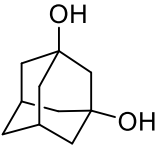
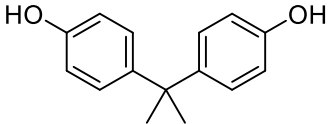


Figure 11. Synthesis of crosslinked polymethylene

2.4.2 Cross-linked polymer gels

To a solution of 200 mg PFA (1.0 eq.) in 200 μ L DMF with the solution of condensation agent (0.05 eq.) in DMF for 1 hour. Then slowly add the DMF solution of cross-linking agent while stirring and observe whether there is solid precipitation or gelation of solution. And there are two types of condensation agents have been attempted, carbonyl diimidazole (CDI) and (1-Cyano-2-ethoxy-2-oxoethylideneaminoxy) dimethylamino-morpholino-carbenium hexafluorophosphate (COMU). CDI is widely used for synthesis of peptides, and it is worth noting that the reaction results in the generation of large amounts of carbon dioxide. COMU is a safer and more efficient peptide coupling reagent and the reaction can be traced by color³⁵. I chose 7 different cross-linking agents for the synthesis and the results are shown in Table 4.

Table 4. Results of cross-linking

Cross-linking agents	Structural formula	Condensation agent (CDI)	Condensation agent (COMU)
1,4-phenylenediamine		Gel	Gel
Hexamethylenediamine		Precipitate	Precipitate
4,4'-Methylenebis(2-methylcyclohexylamine)		Precipitate	Precipitate
1,3-adamantanediamine		Gel	Gel
Cyclohexanedimethanol ^a		Gel	- ^b
1,3-adamantanediol ^a		-	-
Bisphenol A ^a		-	-

^a With 0.02 eq. 4-dimethylaminopyridine (DMAP) as the catalyst.

^b No successful cross-linking into gel

Aliphatic amines are more nucleophilic than aromatic amines since the lone pair of electrons on nitrogen is in resonance in the aromatic ring. Thus, the amidation reaction of aliphatic amines is so easier and faster that polymers precipitate before they form gels. As for the esterification reaction, due to it is much harder to react, I used DMAP as the catalyst to improve the Lewis basicity. However, only the reaction with cyclohexanedimethanol was successful. The reactivity of CDI and COMU can be compared by the time to gel formation. For instance, the cross-linking reaction of 1,4-phenylenediamine formed the gel in 5 minutes with CDI, while it took 2 h to form with COMU. Although it is counterintuitive, it shows that CDI is better suited to this reaction. It may be because COMU has a relatively large steric hindrance, which makes it react less smoothly with the polymer.

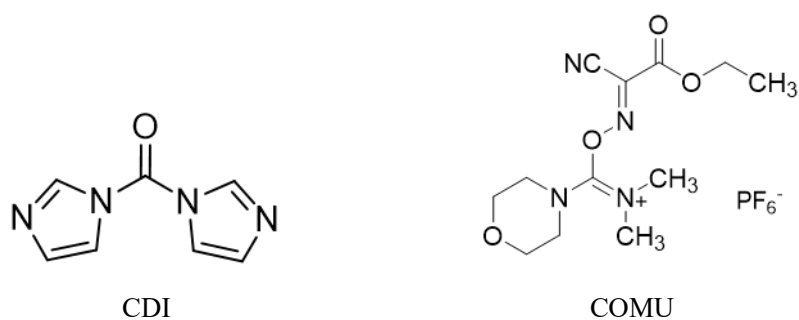


Figure 12. Structure of CDI and COMU

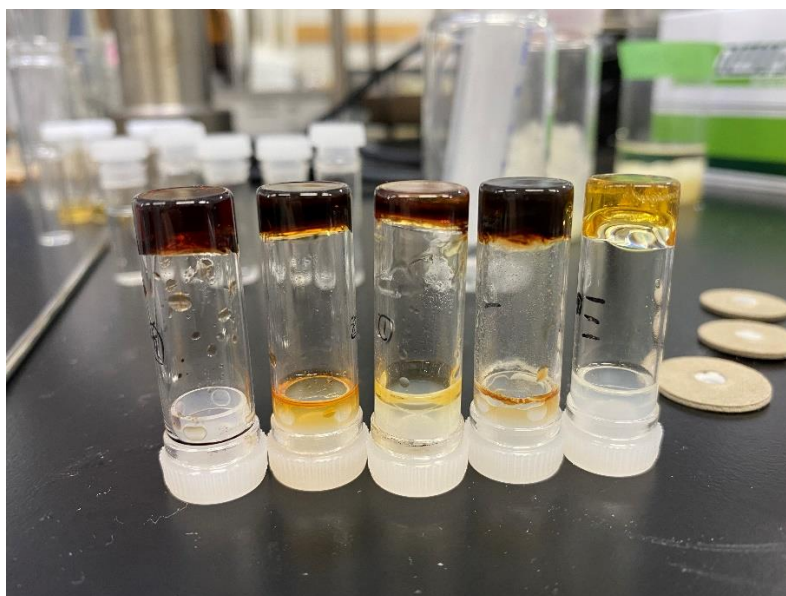


Figure 13. Pictures of gels

CHAPTER 3. CHARACTERIZATIONS OF POLYMETHYLENE

Monomers and polymers are characterized by Nuclear Magnetic Resonance spectroscopy (NMR), Fourier-Transform Infrared spectroscopy (FT-IR), Gel Permeation Chromatography (GPC), Scanning Electron Microscope- Energy Dispersive X-ray Spectroscopy (SEM-EDS), optical microscope and X-ray Diffraction (XRD).

3.1 Nuclear Magnetic Resonance Spectroscopy (NMR)

3.1.1 ^1H NMR spectroscopy

^1H (400 MHz) NMR spectra were measured with JEOL ECS-400 for a CDCl_3 or D_2O solution of sample and are reported in ppm (δ) from internal Me_4Si . As shown in Figure 14, ratio of integral values for poly(ethoxycarbonylmethylene) is a: b: C = 1: 3: 6. As shown in Figure 15, ratio of integral values for di-tert-butyl fumarate monomer is a: b = 1: 9.1, matches molecular formula perfectly. However, due to the peaks of polymer are overlapped, ratio of integral values is calculated by deconvoluted peaks with Lorentzian curve-fitting function. And the result was a: b = 1: 7.9.

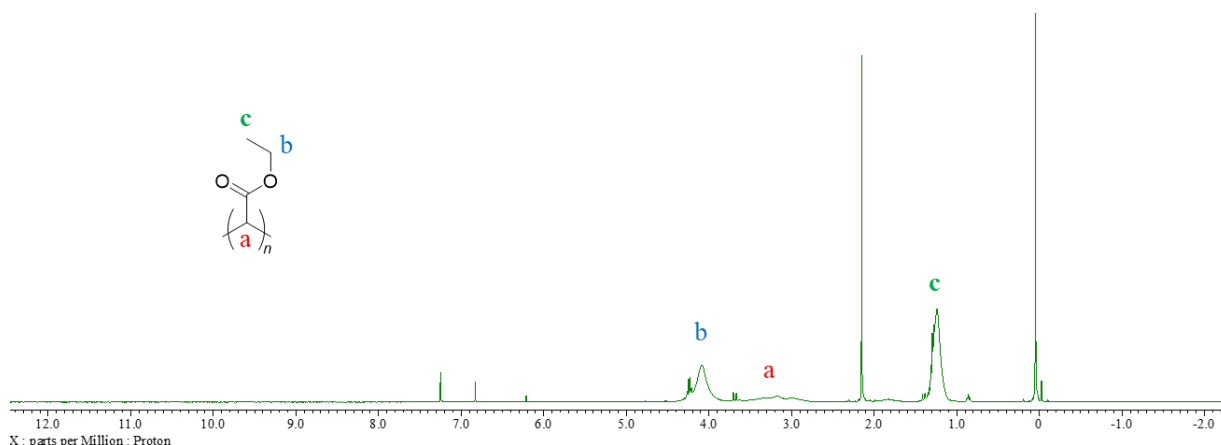
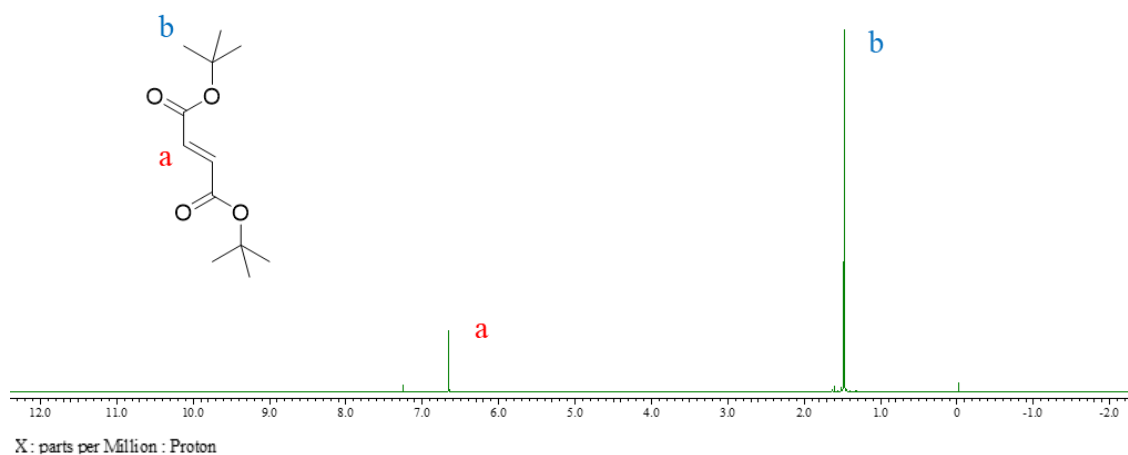


Figure 14. ^1H (400 MHz) NMR spectrum of poly(ethoxycarbonylmethylene) in CDCl_3



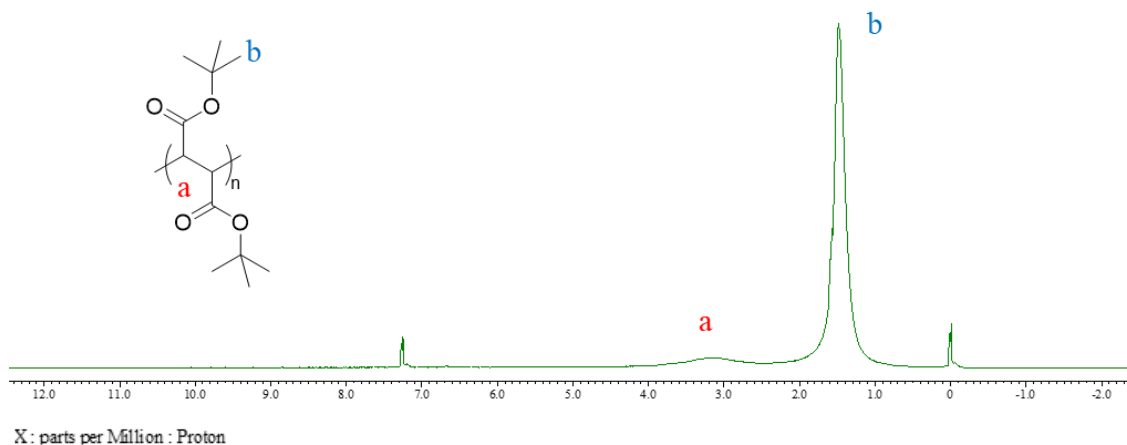
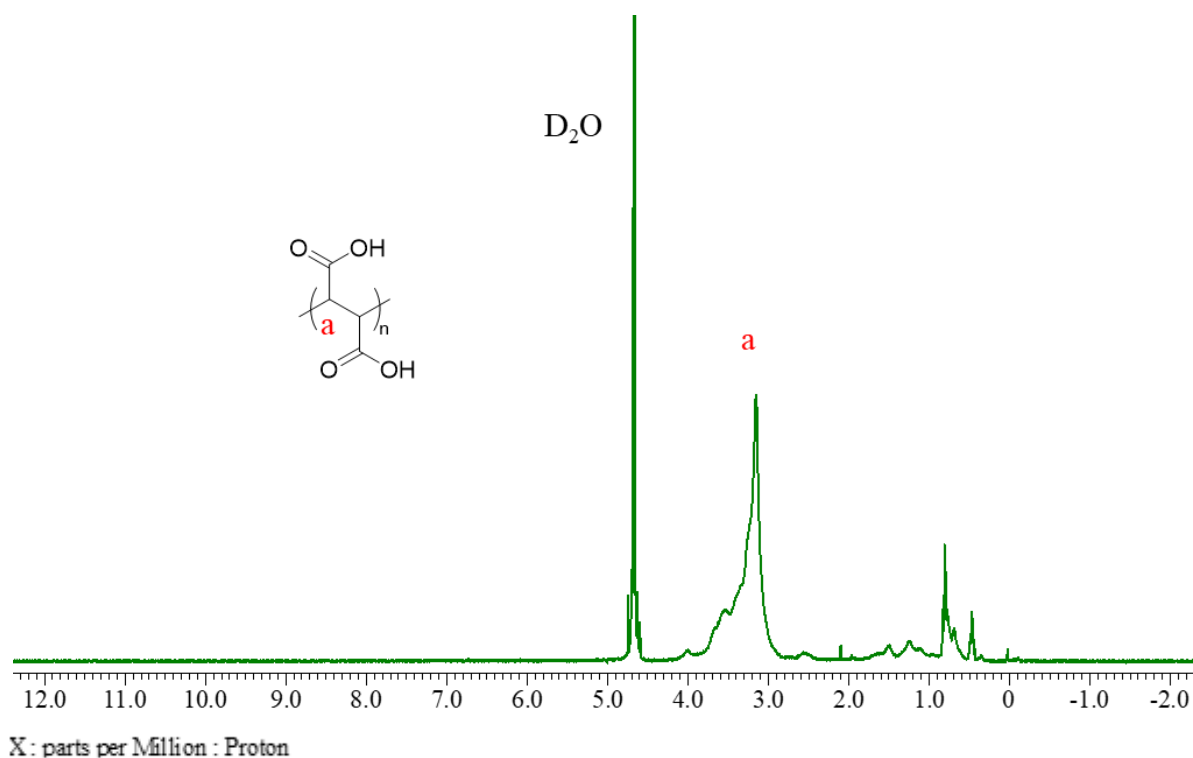


Figure 15. ^1H (400 MHz) NMR spectra of di-tert-butyl fumarate and poly(di-tert-butyl fumarate) in CDCl_3

The spectrum of PFA as shown in Figure 16. There are unidentified peaks may be from water soluble impurities at around 1 ppm. Although the ratio of unknown peaks and mainchain peak calculated by integral value can decrease from 17.5% to 3.9 % by purification, they cannot be removed completely by repeated purification. Hence, we can infer that part of these peaks originate from small molecule or oligomer by-product of pyrolysis reaction. The other peaks may from polymer side chain. The spectra of poly(di-metal fumarate) as shown in Figure 17, the peaks of impurities can still be observed. Hence, I attempted to determine them by ^{13}C NMR spectroscopy.

(a) Unpurified PFA



(b) Purified PFA

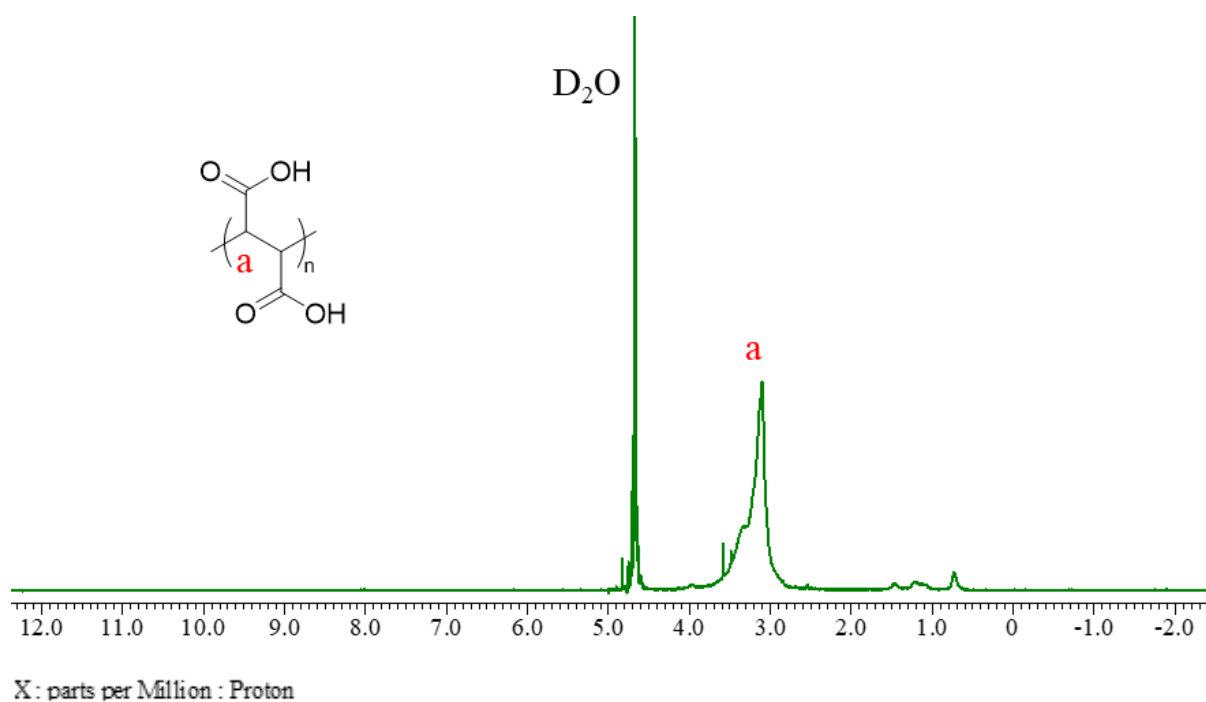
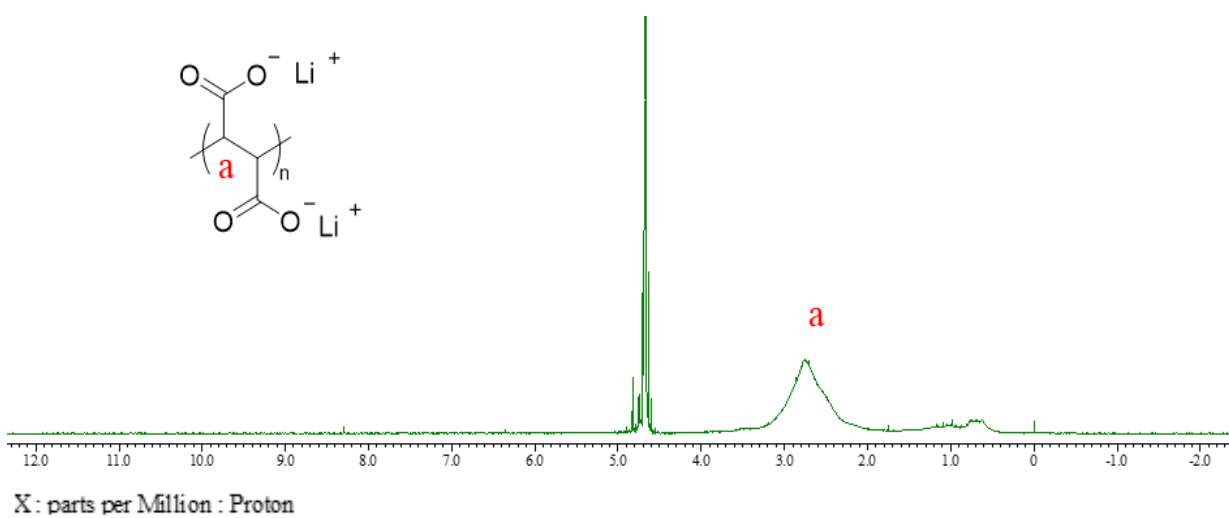
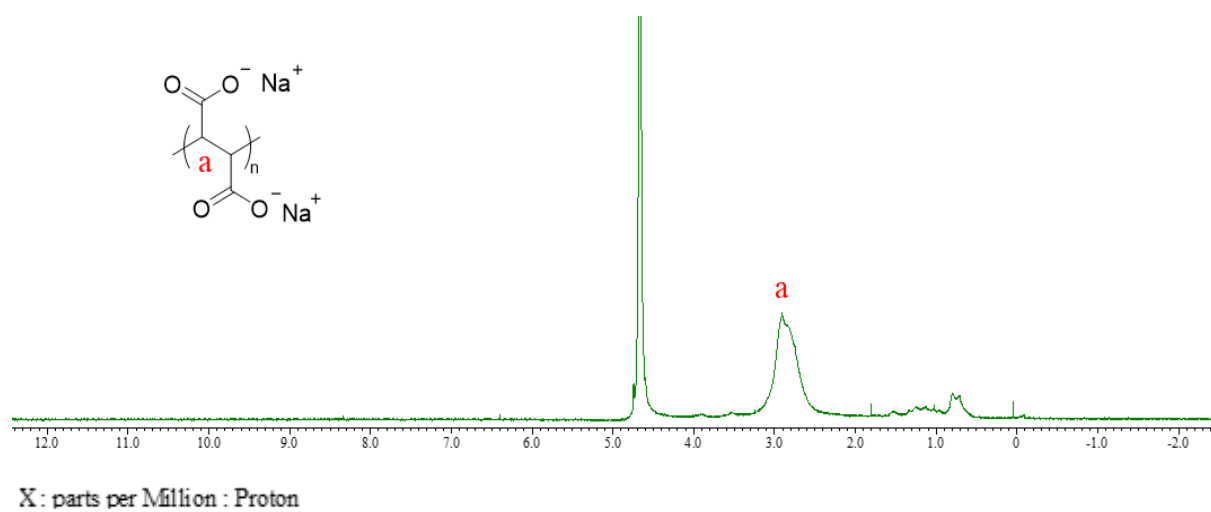


Figure 16. ^1H (400 MHz) NMR spectrum of (a) unpurified PFA, (b) purified PFA in D_2O

(a) Poly(di-lithium fumarate)



(b) Poly(di-sodium fumarate)



(c) Poly(di-potassium fumarate)

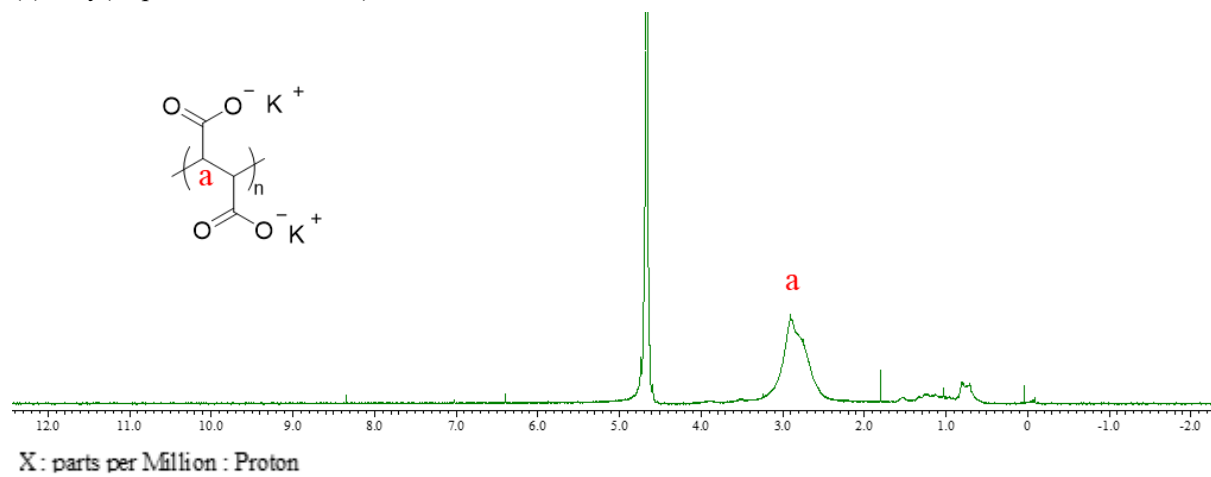


Figure 17. ¹H (400 MHz) NMR spectra of poly(di-metal fumarate) in D₂O

3.1.2 ^{13}C NMR spectroscopy

^{13}C (400 MHz) NMR spectrum and DEPT ^{13}C (400 MHz) NMR spectrum were measured with JEOL ECS-400 for a D_2O solution of sample. Distortionless Enhancement by Polarization Transfer (DEPT) is the most widely used method for determining multiplicities of carbon atoms. Different angles of proton pulse θ is applied, and the spectra on comparison with the broad-band decoupled spectrum suffice to identify CH_3 , CH_2 , CH , and quaternary carbons. With θ at 45° , all protonated carbons (CH_3 , CH_2 , and CH) appear with positive phases. With θ set at 90° , only CH carbons are recorded. With θ at 135° , the CH and CH_3 carbons give positively phased signals and CH_2 carbons give negatively phased signals so that CH_3 and CH carbons are modulated differently from CH_2 carbons. Signals at each angle with different carbons are summarized in Table 5.

Compared to the ^{13}C (400 MHz) NMR spectrum of PFA shown in Figure 18, there is only one peak at all of angles in the DEPT ^{13}C (400 MHz) NMR spectrum of PFA shown in Figure 19. So that it can be considered that the peak at around 45 ppm is a CH carbon. Peaks at 175 ppm is a quaternary carbon because it only can be observed in Figure 18. Corresponding to PFA, this CH carbon is the carbon in mainchain, and the quaternary carbon is the carbon in carboxyl group. As for the peaks of impurities mentioned above, the signal is too weak to identify clearly. But we are still able to find several peaks at 12, 20, 30 ppm in Figure 18, and peaks only at 90° spectrum in DEPT cannot be observed clearly. Hence, there is a high probability that these peaks are CH_3 and quaternary carbon. The question is does these peaks in ^{13}C NMR spectrum correlate with those unidentified peaks in ^1H NMR spectrum.

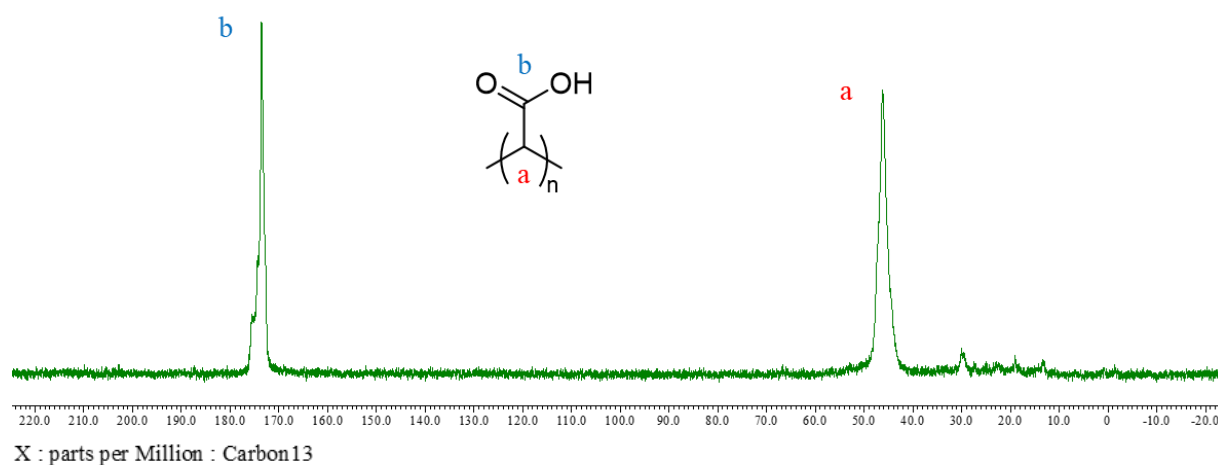


Figure 18. ^{13}C (400 MHz) NMR spectrum of PFA in D_2O

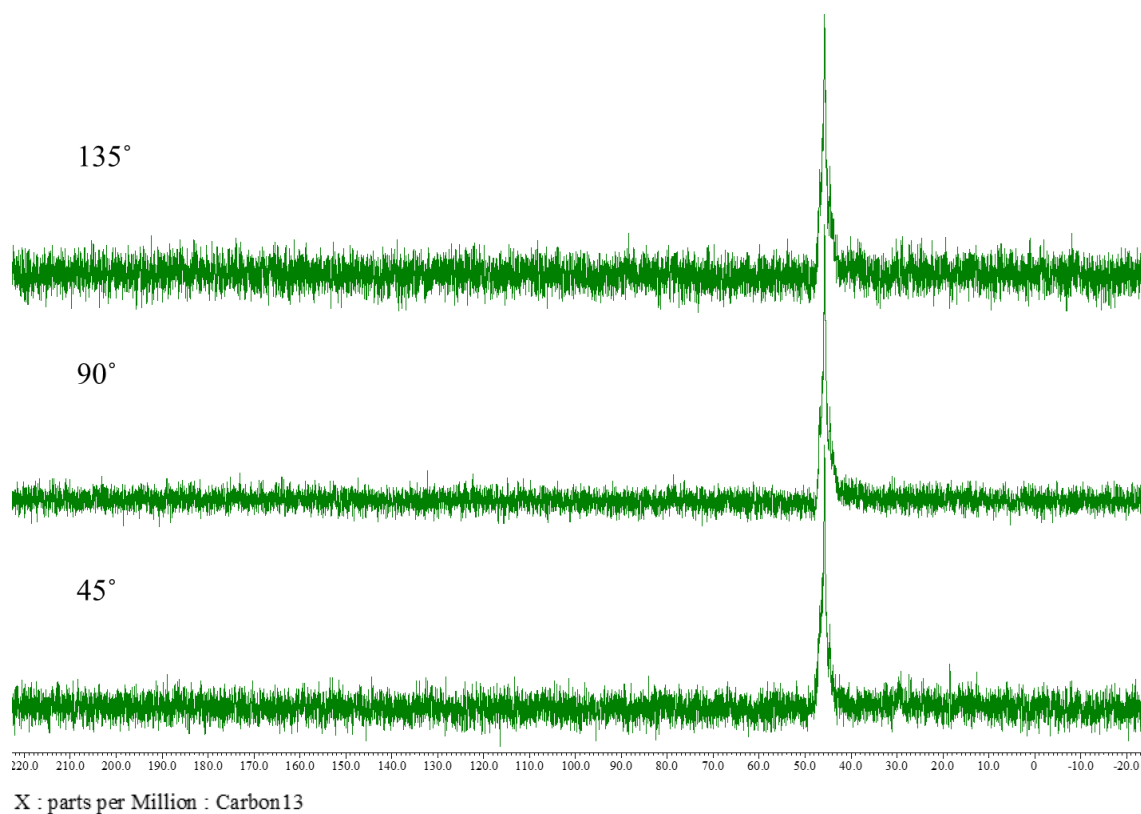


Figure 19. DEPT ^{13}C (400 MHz) NMR spectrum of PFA

Table 5. Signal orientation at each angle

θ	CH_3	CH_2	CH	C
45°	⊥	⊥	⊥	-
90°	-	-	⊥	-
135°	⊥	⌞	⊥	-

⊥: positive phase signal

⌞: negative phase signal

-: no signal

3.1.3 Heteronuclear Multiple-Quantum Correlation

The 2D Heteronuclear Multiple-Quantum Correlation (HMQC) experiment permits to obtain a 2D heteronuclear chemical shift correlation map between directly bonded ^1H and X-heteronuclei commonly ^{13}C and ^{15}N . We can determine that carbons are directly or remotely attached to protons by HMQC.

As the spectrum shown in Figure 20, we can see that carbon in mainchain (C_a) correlate with hydrogen in mainchain (H_a), and there is no proton correlate with carbon in carboxyl group (C_b). There are only signals between proton at around 1 ppm and carbon at 30 ppm, that means they are correlated. According to the spectra above, we can summarize that part of unidentified peaks are from polymers and the structure probably is t-butyl group that from the prepolymer PDtBF.

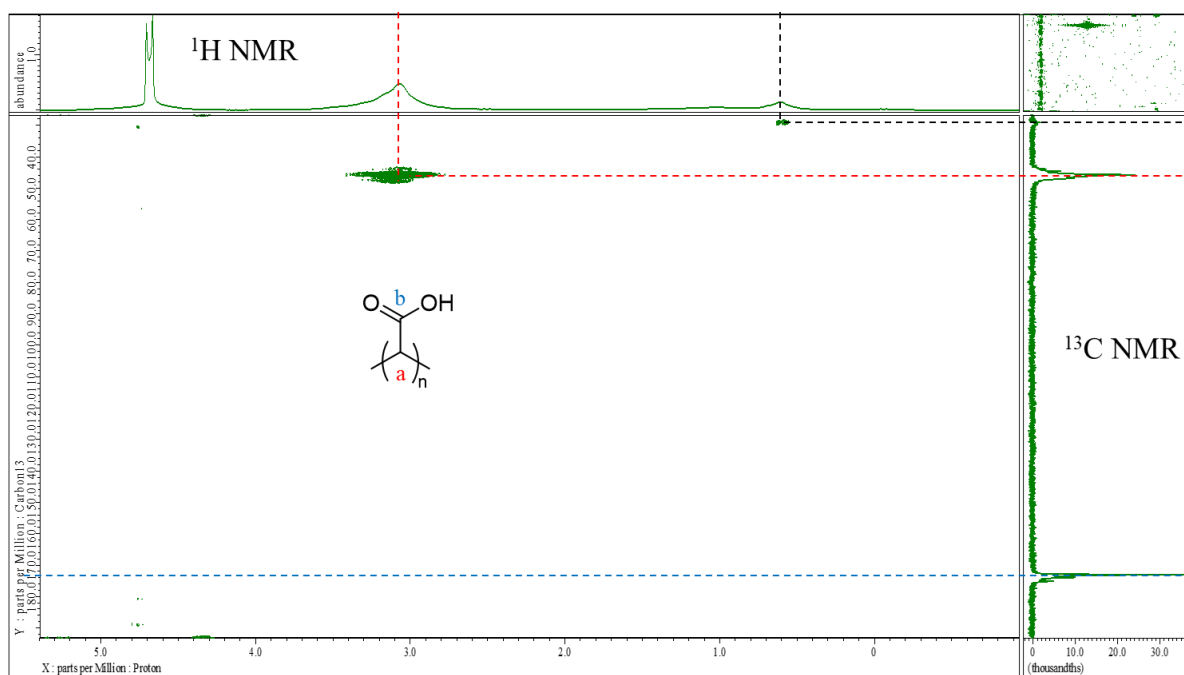


Figure 20. HMQC spectrum of PFA

3.2 Gel Permeation Chromatography (GPC)

Gel permeation chromatography (GPC) was performed with Viscotek TDA 302 or JASCO EXTREMA system equipped with polystyrene mixed gel columns at 40 °C using RI and viscosity detectors, and THF and DMF as an eluent. The weight-average molecular weight (M_w) and the number-average molecular weight (M_n) were calculated and calibrated with PMMA standards.

The injection solution was prepared by dissolving 5 mg PDtBF in 1 mL THF and filtered through a 0.45 μ m filter before injection. The injection solution of PFA was prepared by the same method in DMF. A set of data of molecular weights is shown in Table 6 as an example. According to theoretical calculations, the molecular weight of PFA produced by PDtBF after pyrolysis is about 50% of the original. The experimental results are inconsistent with the theory for two reasons: 1) Because PFA is no longer soluble in THF, and there is no solvent that dissolves both PDtBF and PFA well, different gel columns and eluents are used, and the result of calibration would be different. 2) When analyzing polar polymers using DMF as an eluent, the apparent molecular size may increase due to the repulsion between ionic groups in the polymer molecule and the expansion of the molecule or the association. In a summary, molecular weight of PFA measured by GPC as DMF eluent is inaccurate. Its approximate molecular weight can be inferred from PDtBF.

As for the poly(ethoxycarbonylmethylene) which synthesized by C1 polymerization, the M_n is around 2000, and M_w / M_n is 1.42. Compared to the free radical polymerization of di-tert-butyl fumarate, the molecular weight of this polymer is too small. To ensure its thermal stability, a polymer molecular weight greater than 10,000 is preferable.

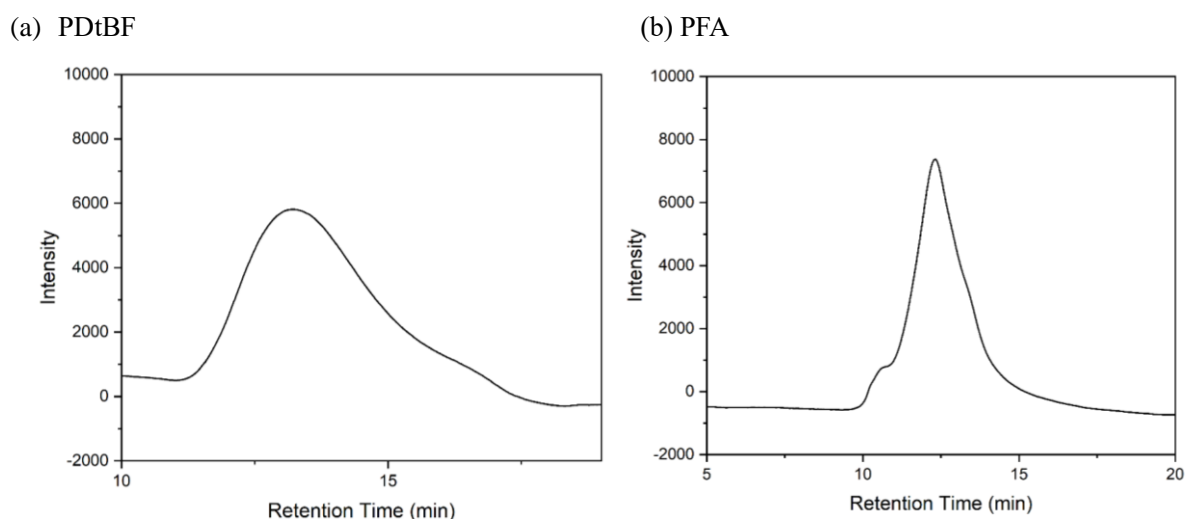


Figure 21. GPC trace of PDtBF and PFA

(a) PDtBF (b) PFA

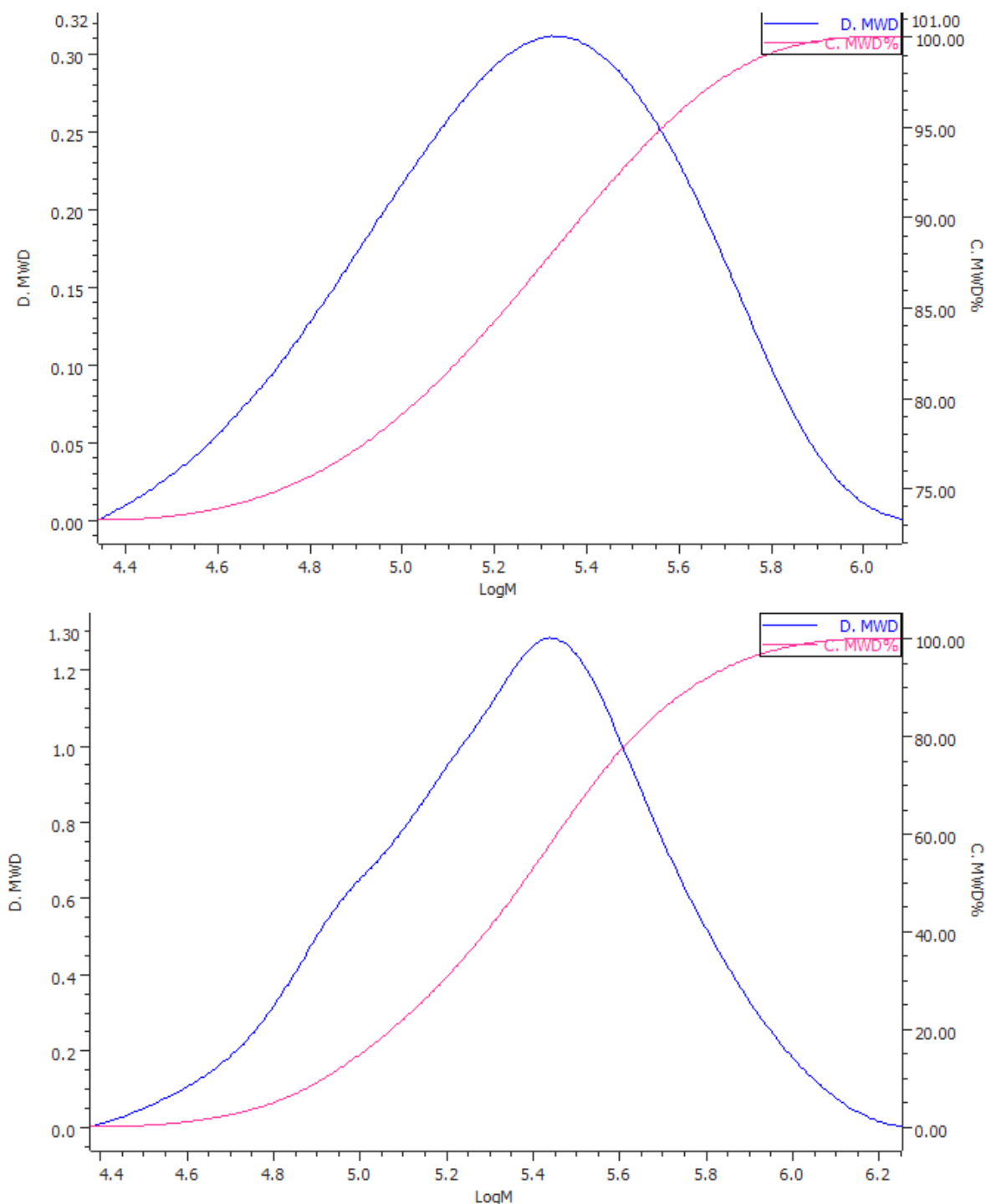


Figure 22. Molecular weight distribution curve of a) PDtBF b) PFA

Table 6. Molecular weight measured by GPC

	$M_n \times 10^{-4}$	$M_w \times 10^{-4}$	M_w / M_n
PDtBF	13.8	23.6	1.7
PFA	17.2	29.7	1.7

3.3 Fourier Transform Infrared Spectroscopy (FT-IR)

IR spectra were measured by JASCO FT/IR-6100 with KBr pellet. As shown in Figure 23, the strong absorption of stretching vibration of carbonyl group can be observed at 1720 cm^{-1} . And there are characteristic bands at 1850 cm^{-1} and 1780 cm^{-1} for the stretching vibration of the anhydrous carbonyl group both in PFA before and after purification, but these bands are weakened in pure PFA. Besides, PFA is yellow powder which can dissolve in water, N,N-dimethylformamide, acetonitrile, methanol, acetone, and some other polar organic solvents easily before purification. It becomes a colorless powder and is only soluble in water, but insoluble or requires heating to dissolve in other polar organic solvents after purification. The characteristic bands of the anhydride disappeared completely and there is only asymmetric stretching vibration of carboxylate at 1580 cm^{-1} after the neutralization with the base as shown in Figure 23. Therefore, we consider that a side reaction of dehydration between carboxyl groups to form anhydride occurred during the preparation of PFA using pyrolysis. Although we can still see part of the characteristic bands in the pure PFA, indicating that it is relatively stable and is not completely hydrolyzed in aqueous solution at room temperature. This does not affect our evaluation of the thermal and transmission properties of poly(di-metal fumarate), because the neutralization or hydrolysis in base is completely. It is noted that if I measure same samples by Attenuated Total Reflection (ATR) FT-IR, the intensity of spectra will be weak and the characteristic bands of carbonyl group shift to around 1600 cm^{-1} .

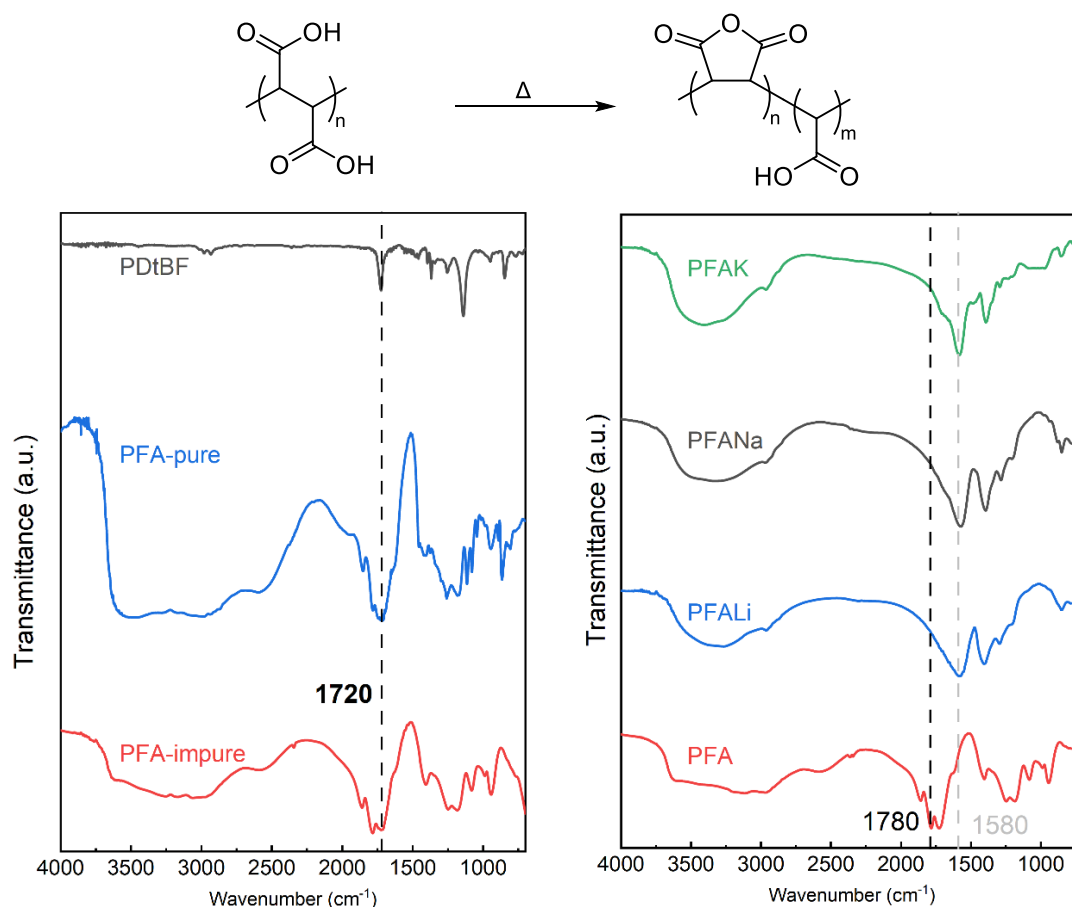


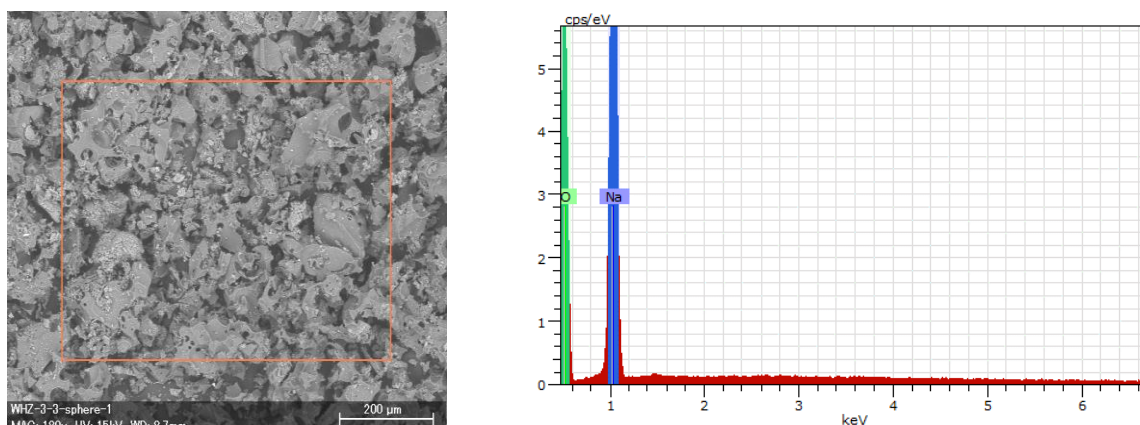
Figure 23. IR spectra of polymers

3.4 Scanning Electron Microscope- Energy Dispersive X-ray Spectroscopy (SEM-EDS)

Scanning Electron Microscope- Energy Dispersive X-ray Spectra was performed on Hitachi TM3000. Specimens of hydrolysis product was prepared by cracking solid precipitation of reaction. According to the images of elements distribution as shown in Figure 24. We can find that the three main elements of the hydrolysis products (hydrogen cannot be observed by EDS) have the same distribution in the sample. This indicates that the sodium salt can indeed be produced by the hydrolysis reaction.

The product of neutralization as shown in Figure 25, specimens are prepared by adding PFA-Na solution dropwise on a glass plate and dried at room temperature, 50°C, 70°C. The purpose of observing this by SEM was to investigate why only the sodium salt was poorly soluble, and whether the precipitation formed a partial crystallization or a molecular packing. The SEM images are bright and not clear probably because its conductivity is not good enough on glass. We can find a lot of needle-like substances in the samples dried at 70 °C and 50 °C, and regular arrangement in some areas can be observed in the samples dried at room temperature. To further determine the structure of the polymer, I also characterized it by optical microscopy and X-ray diffraction spectroscopy.

(a) SEM image of crushed powder-like sample. (b) EDS spectrum of product of hydrolysis



(b) Images of elements distribution.

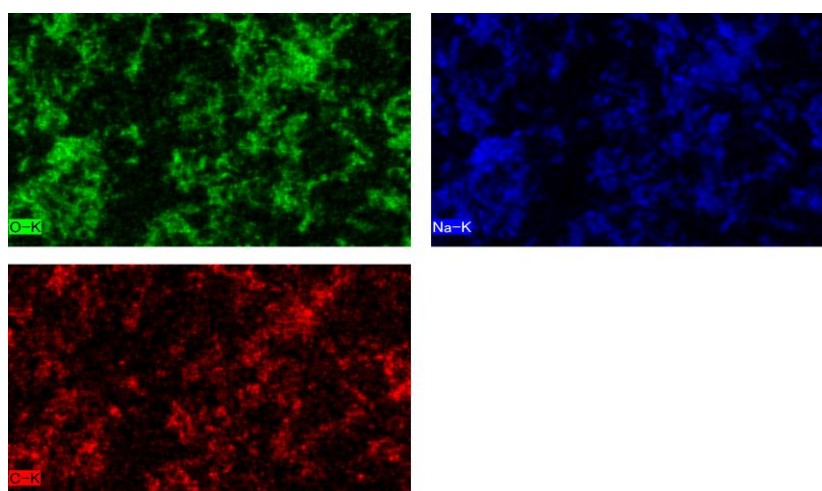
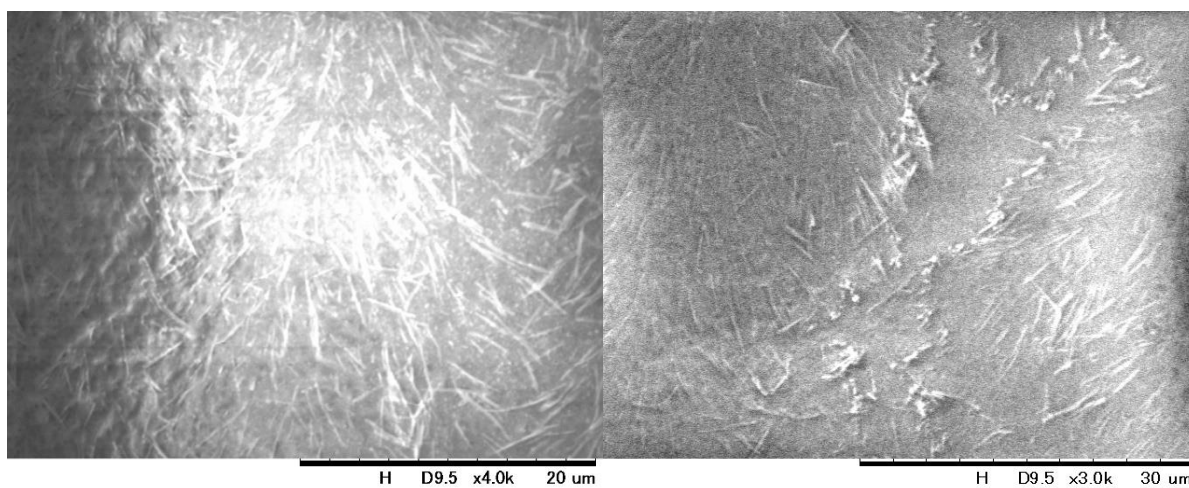
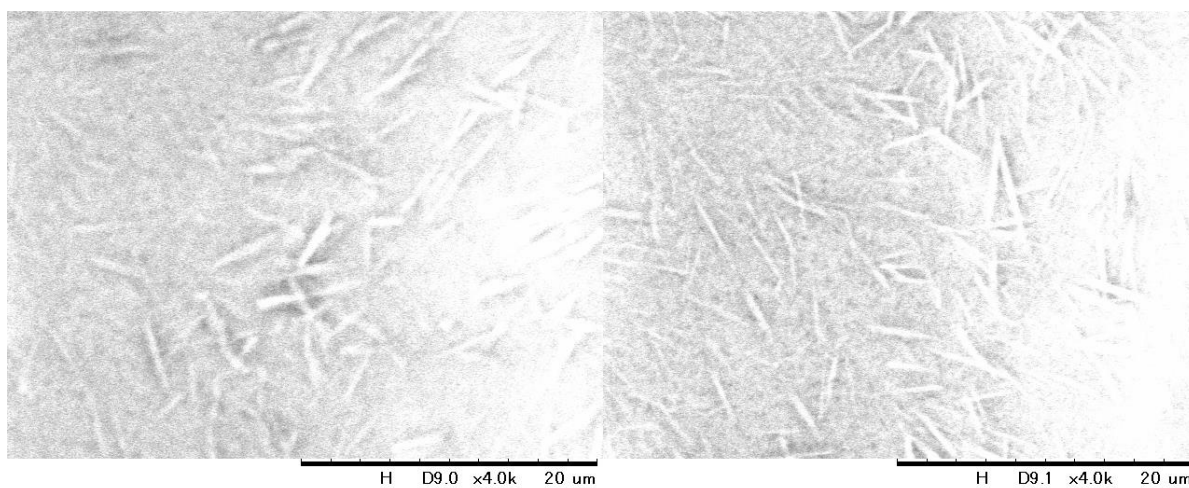


Figure 24. SEM-EDS spectrum of product of hydrolysis. Images of elements distribution.

(a) Dried at 70 °C



(b) Dried at 50 °C



(c) Dried at room temperature

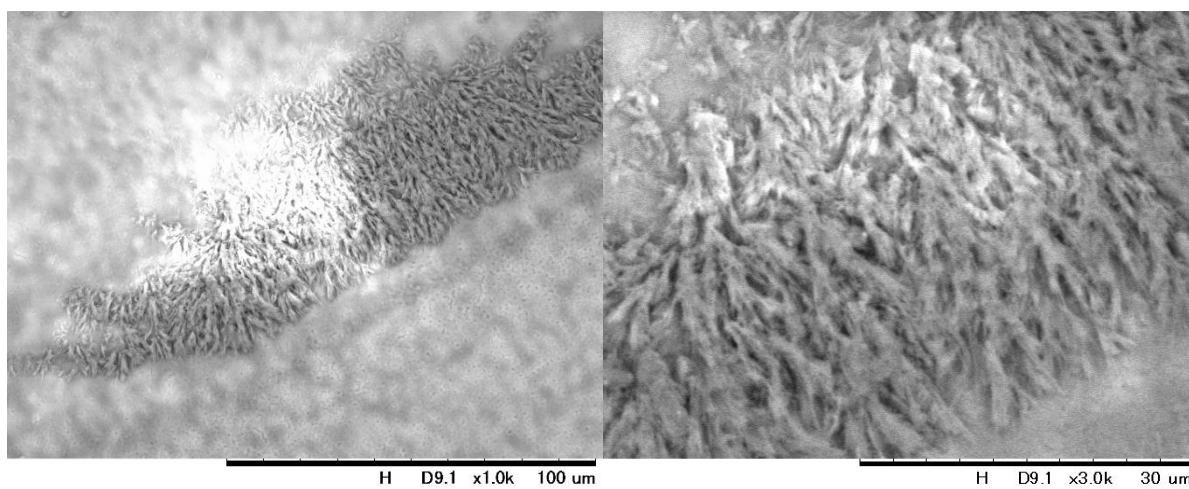


Figure 25. SEM images of PFA-Na dried at different temperatures

3.5 Optical Microscope

Samples are prepared by the same method in 3.4, solution of PFA, PFA-Li and PFA-K are also used in this measurement and pictures are shown in Figure 26. Among them, PFA-Na shows interesting morphology. As shown in Figure 27, for the samples of PFA-Na dried at 50 °C and room temperature, we can see that the crystalline precipitation is arranged in rings, and that the rings are separated by a relatively uniform distance from each other. The radial arrangements can be observed in each layer of rings. As shown in Figure 28, these pictures were taken in different positions on the sample, and the magnification of the first and second one is 560 times while the third one is 140 times. Interestingly, the polymer arranged like branches, that indicated PFA does not form a film of amorphous polymers, but a layer of precipitation dispersed on the glass plate. Besides, for the orientation of polymer arrangement, the first picture differs from the second one and we can see a clear boundary at the junction of the branches in different directions. These images demonstrated that PFA-Na solids possibly assembled at different temperatures and rates of drying to form different aggregates. The study of PFA-Na solid aggregation will be further explored in the next studies.



Figure 26. Polymer films on glass plate

a: PFA-Na dried at 50 °C

b: PFA-Na dried at room temperature

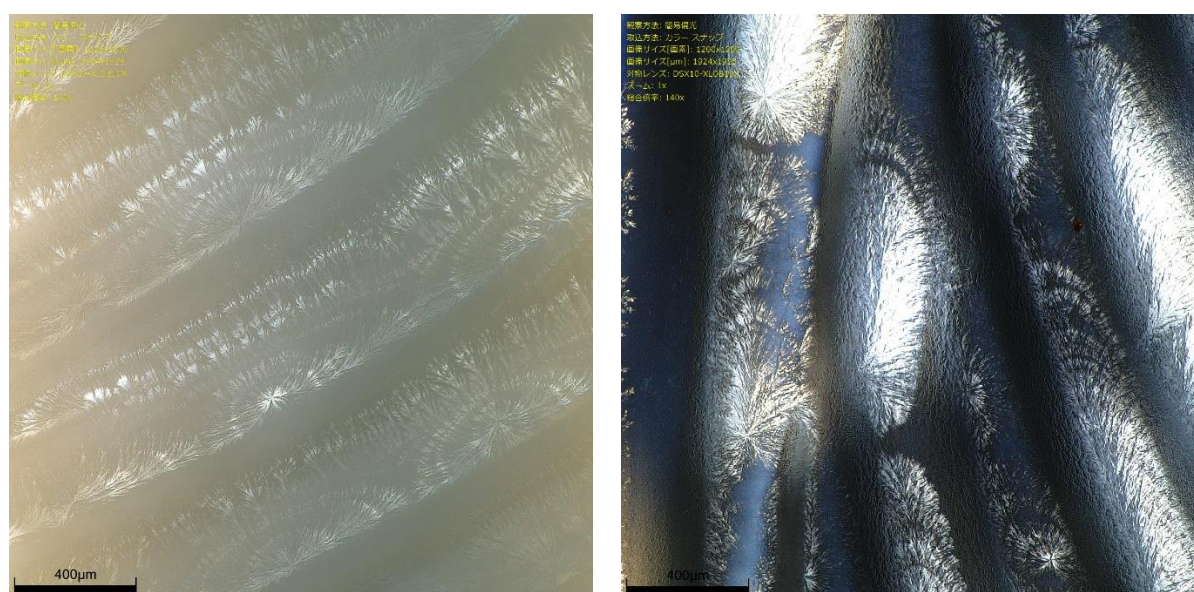


Figure 27. Images of PFA-Na dried at 50 °C and room temperature

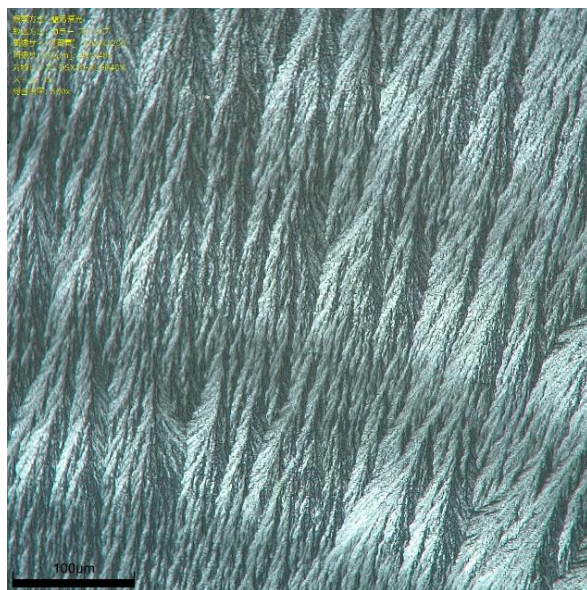


Figure 28. Images of PFA-Na dried at 70 °C

3.6 X-ray Diffraction (XRD)

XRD was performed by MiniFlex600 (RIGAKU) using 40kV, 15mA, Cu K α radiation ($\lambda = 1.5405\text{\AA}$) with a scan speed of $2\theta = 5 \text{ deg./min}$ in the scan range from 2 deg. to 60 deg. . As shown in Figure 29, the diffraction peak of PDtBF can be observed in XRD pattern while there are only amorphous halos for PFA-Na and PFA-Li. The rigid main chain of PDtBF possibly assembled to form any aggregates present in the solid-state. However, the alignment of PFA-Na observed by SEM is not reflected in the XRD pattern. It may be because the powdered sample destroys the structure, or the sample does not have a crystal structure at all.

The d values are calculated from the position of the diffraction peak by Bragg's law. Both PDtBF and PFA-Na have 1,2 disubstituted repeating units, differing only in the end of the substituent. However, as shown in Table 7 and Table 8, due to the different sizes and chemical properties of the tert-butyl and metal ions, they show different diffraction angles and d values. It is indicated that the rigidity of substituent polymethylene, changed with the introduction of metal ions. The exact change in rigidity will be investigated in the next study.

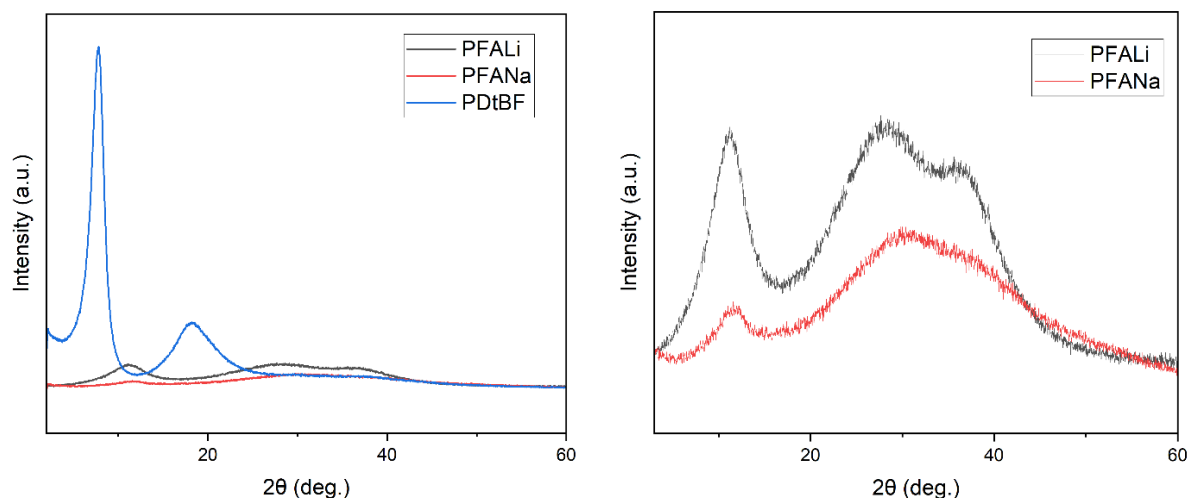


Figure 29. XRD patterns of PDtBF, PFA-Li and PFA-Na

Table 7. X-ray diffraction data for PDtBF

2θ (deg.)	d value (\AA)
7.80	11.3
18.1	4.90

Table 8. X-ray diffraction data for PFA-Li and PFA-Na

2θ (deg.)	d value (\AA)
11.3	7.86
27.7	3.22
37.1	2.42

CHAPTER 4. THERMAL AND OPTICAL PROPERTIES OF POLYMETHYLENE

4.1 Thermal analyses

4.1.1 Thermal gravimetric(TG) analysis

Thermogravimetric (TG) analysis was performed on Hitachi TG/DTA7300, and measurements were obtained under a nitrogen stream at a heat rate of 10°C/min with aluminum pan. In the temperature program for TG, the temperature was kept at 150°C for 5h before further temperature rising to 500 °C to remove the adsorbed water in the sample. The thermal decomposition temperature (T_d) was determined to be the temperature at which 5% weight loss. DTG is the percentage of weight loss per minute, which reflects at which temperature interval the mass loss is most severe.

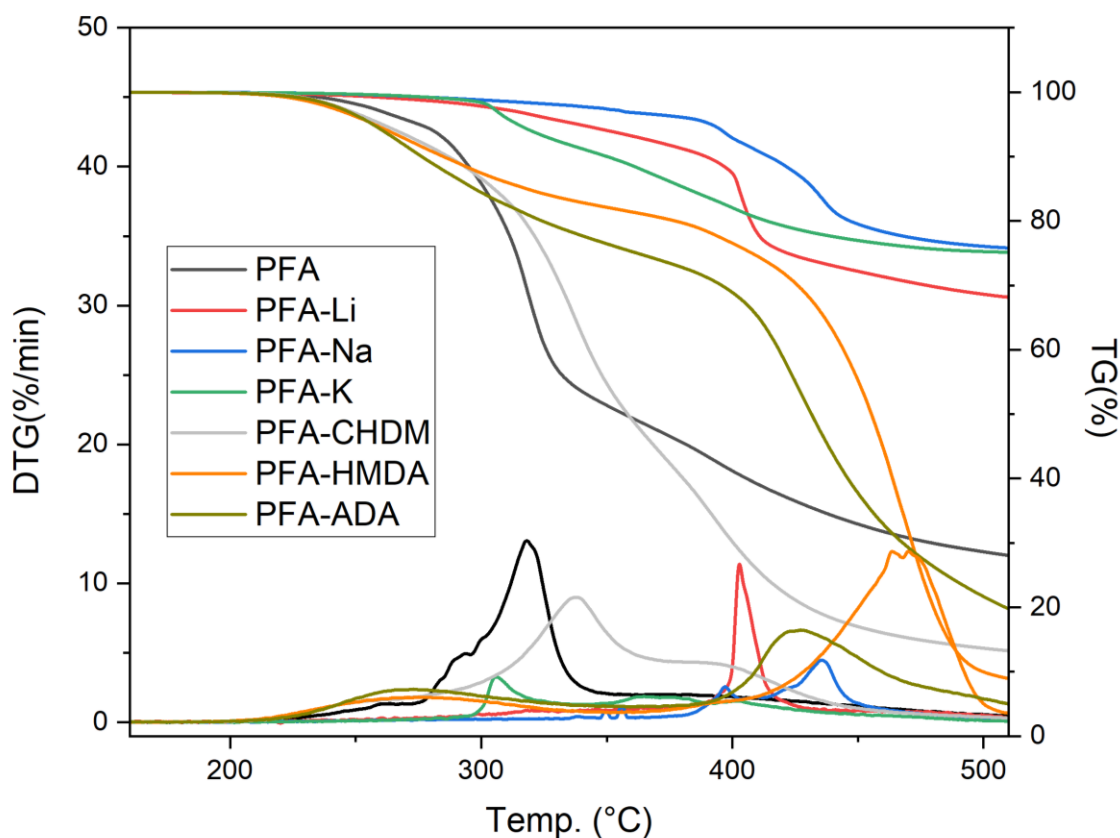


Figure 30. TG and DTG curves of polymers

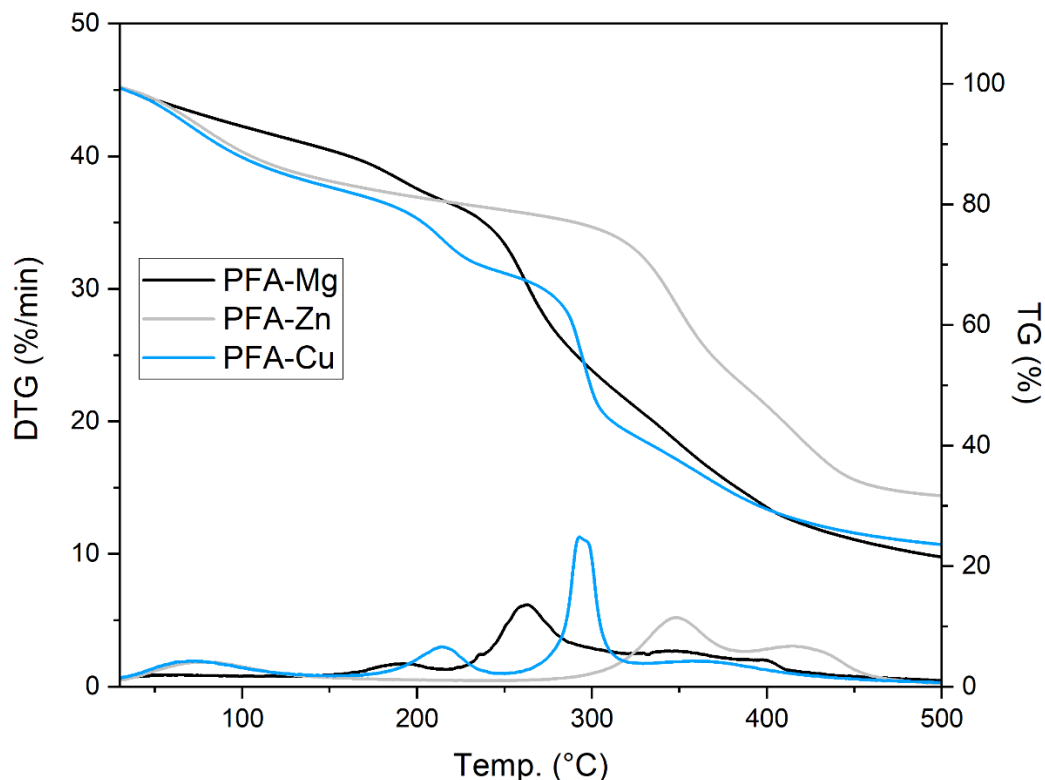


Figure 31. TG and DTG curves of PFA-Mg, PFA-Zn and PFA Cu

Table 9. Thermal decomposition temperatures of polymers

Polymers	$T_d / ^\circ\text{C}$
PFA	276
PFA-Li	343
PFA-Na	384
PFA-K	298
PFA-CHDM	252
PFA-HMDA	249
PFA-ADA	249

As shown in Figure 30, PFA and the onset temperature of thermal decomposition for PFA salts is higher than PFA and cross-linked polymers. One of the reasons is thought to be the difficulty in purifying the cross-linked polymer and the lack of assurance that all cross-linking agents and condensation agents are removed. And the dehydration of PFA mentioned in 3.3 also led to early weight reduction. The salts do not have these problems, so their thermal decomposition temperature is much higher than the others.

As for the salts with monovalent ion, sodium salt has the highest T_d . They have different residual weight percentage because of metal ions do not change into gaseous substances to leave at the measurement temperature. According to calculations, if all these metal ions are left in the form of carbonates, the percentage of mass of the residue is approximately 58% to 74% of the original. This is substantially the same as the

experimental results, and the reason for the difference may be that the decomposition of polymer salts to carbonate is not complete at the measurement temperature with aluminum pan. It is worth noting that we can find the temperature of the fastest mass loss from the peaks in the DTG curve. This can be considered as the temperature at which the most significant thermal decomposition occurs. The position of the peaks in the DTG curves of different polymers differs due to the different energies of the chemical bonds that constitute their side chains.

As shown in Figure 31, PFA with divalent ions also do not remove all the mass until 500°C. Unlike alkali metals, the carbonates of these divalent ions can decompose to metal oxides at relatively low temperatures. However, even assuming that all the metal is converted to oxide, the remaining mass is less than the calculated value. The reason could be that there is water of crystallization in the sample that cannot be removed, or that the reaction is incomplete due to rapid precipitation formation of polymers during the preparation process.

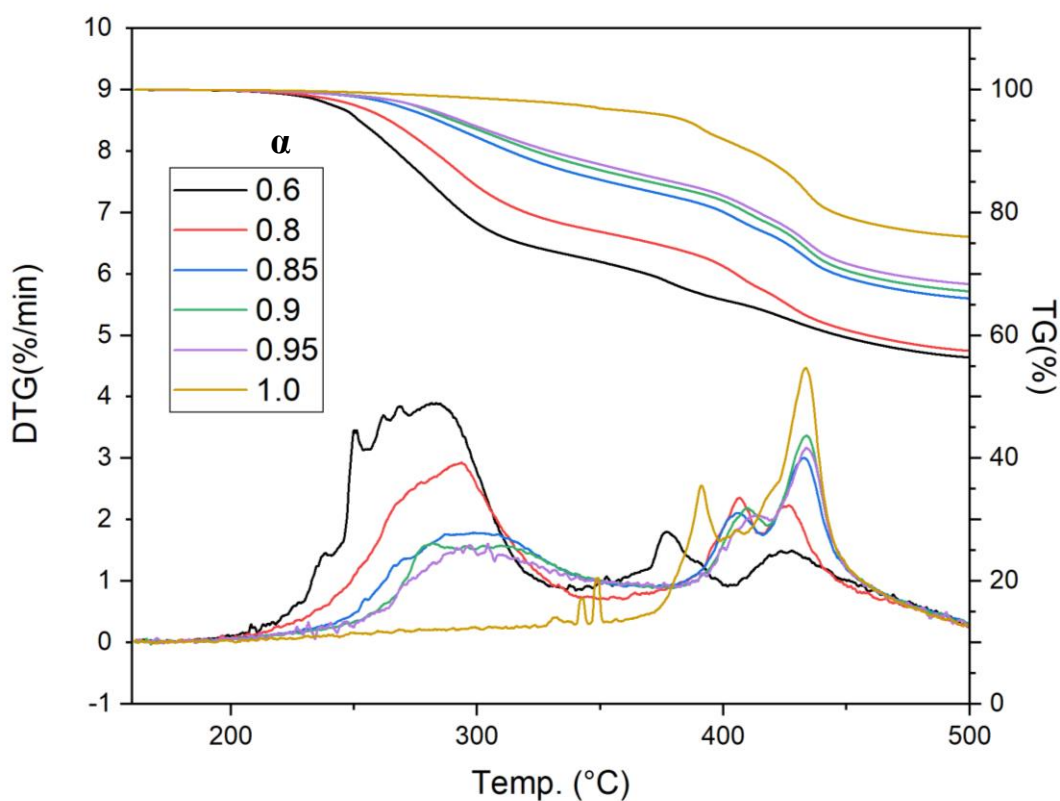


Figure 32. TG and DTG curves of PFA-Na in different degree of neutralization (α)

$$\alpha = \frac{n(\text{NaOH})}{n(-\text{COOH})}$$

n: Amount of substance

Table 10. Thermal decomposition temperatures of PFA-Na with different α

α	$T_d / ^\circ\text{C}$
0.6	252
0.8	267
0.85	284
0.9	290
0.95	293
1.0	384

As shown in Figure 32 and Table 10, the T_d of PFA-Na increases with the degree of neutralization (α). DTG curves shows a significant mass loss of PFA-Na around 300 °C, which implies that a decomposition occurs near this temperature. Moreover, the percentage of mass loss, which is the height of this peak, decreases with increasing α . In the sample with the α of 1.0, where all the carboxyl groups were neutralized with sodium hydroxide, the peak almost disappeared. Therefore, I inferred that this decomposition is related to carboxyl groups.

As I discussed above in 2.3.4, PFA-Na in different α also shows different solubility and ability of film formation. The boundary is $\alpha = 0.8$. When $\alpha < 0.8$, PFA-Na can dissolve in water and form films by drying from aqueous solution. When $\alpha > 0.8$, it is still soluble in water, but no longer able to form films. Therefore, PFA-Na can meet the needs of different fields by changing α .

Although the T_d of PFA salts is not very good among all polymers, the advantage of these polymers is that there is no T_g . That is, the physical and chemical properties do not change significantly until their decomposition temperature. We can compare the T_d of PFA salts with the T_g of other materials.

4.1.2 Differential scanning calorimetry (DSC)

Differential scanning calorimetry (DSC) was measured on Shimadzu DSC-60Plus under nitrogen atmosphere. The sample was heated at 200 °C for 10 min to erase thermal history, then cooled down, and the temperature cycle was applied at a rate of 10 °C/min. According to the results in TG analysis, the maximum temperature of DSC should be at least 50 °C lower than the thermal decomposition temperature of polymers. As shown in Figure 33, T_g cannot be observed for all these polymers. It can be considered that their T_g is higher than their T_d . A weak step can be observed around 80-90 °C in the DSC curve of PFA. According to the research for poly(fumarate) which have similar structure with PFA³⁶⁻³⁸, β relaxation of poly(fumarate) are determined at 80°C. In most cases, only the α relaxation shows a detectable change of heat capacity. However, the precise measurement of heat can detect β relaxation as well.

Although these polymers do not have T_g , it can be considered that the mechanical properties of materials do not change significantly up to the thermal decomposition temperature. It is acceptable as a heat-resistant material.

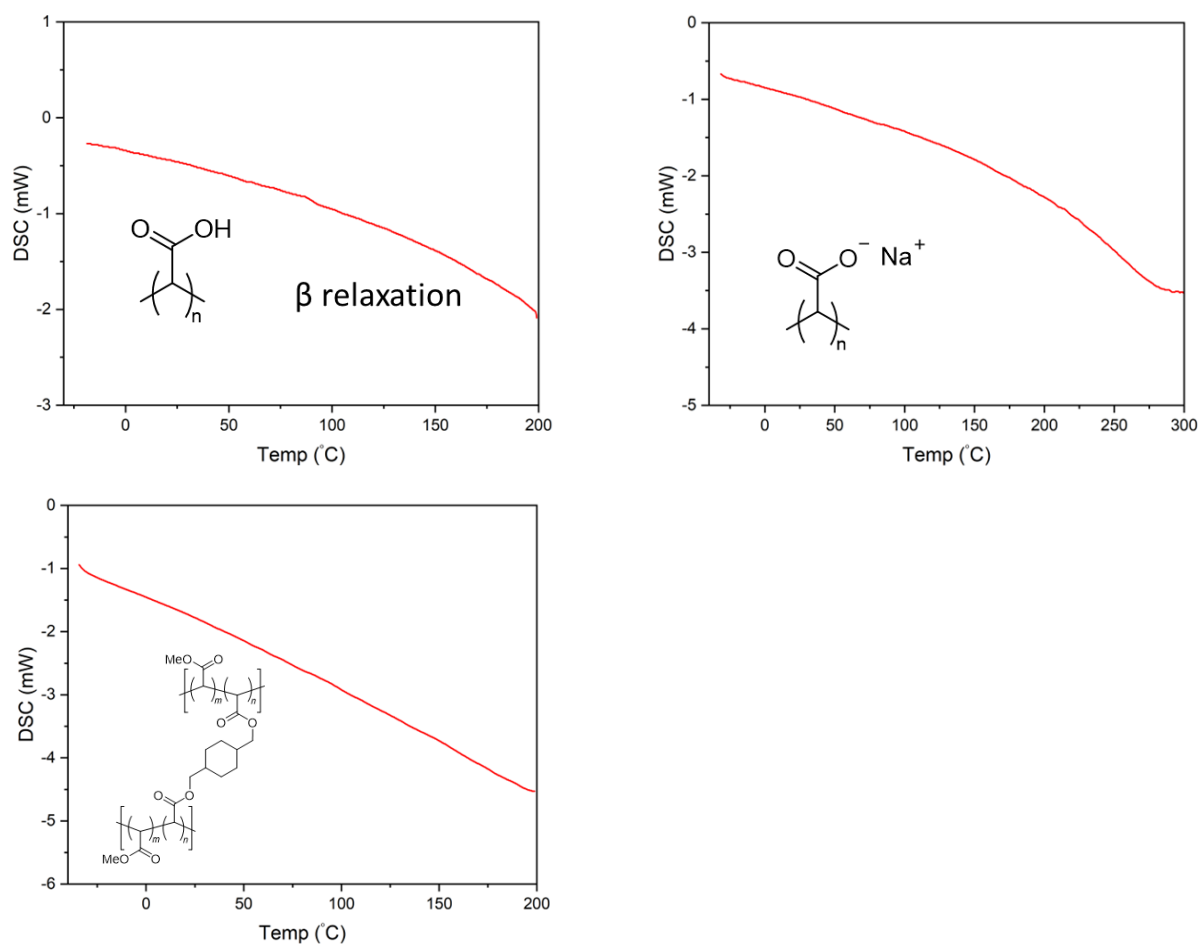


Figure 33. DSC curves of polymers

4.2 Transmittance measurements

4.2.1 UV-vis spectroscopy

UV-vis spectra were measured in the wavelength (λ) range from 200 nm to 800 nm with JASCO V-600. As shown in Figure 34, samples are prepared on the surface of quartz cell by drying from solution of polymers and the thickness of films are measured by micrometer screw. Since the cross-linked polymers are insoluble in any solvent and difficult to be processed into films, only the transmittance of PFA salts is measured. As shown in Figure 35, there is an absorbance can be observed at around $\lambda = 200$ nm. Generally, UV spectra of organic carboxylic acids and their salts have two main bands ascribed to $-\text{COOH}$ ($n \rightarrow \pi^*$, $\lambda_{\text{max}} = 210$ nm) and to $-\text{COO}^-$ ($\pi \rightarrow \pi^*$, $\lambda_{\text{max}} = 183$ nm) which is the same for polymers³⁹⁻⁴¹. There is no absorption peak in the visible region, but the scattering of light by the sample due to the poor film forming ability of sodium and lithium salts leads to a transmittance of 60-80%. Therefore, I measured polymers by haze meter to exclude the influence of scattered light.



Figure 34. Pictures of polymer film for transmittance measurement

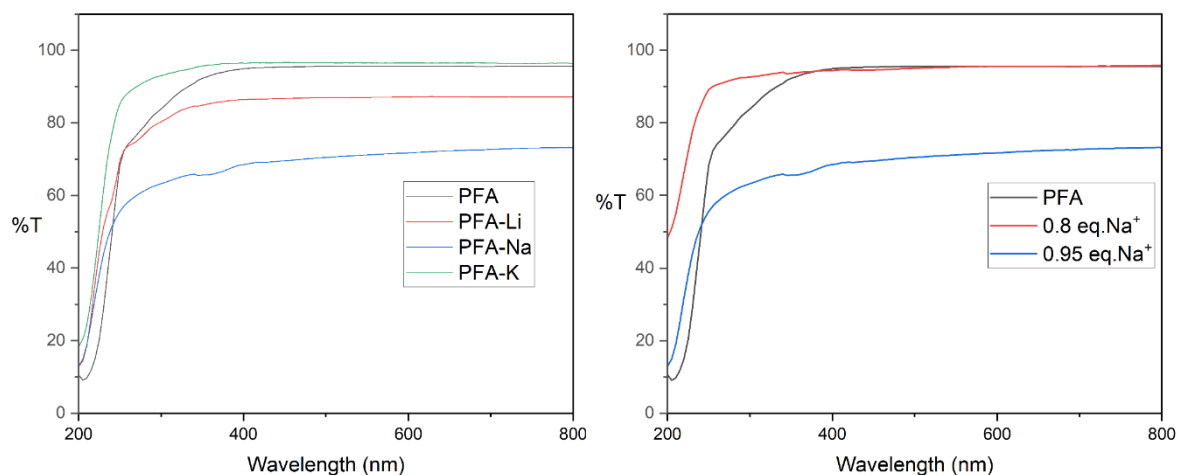
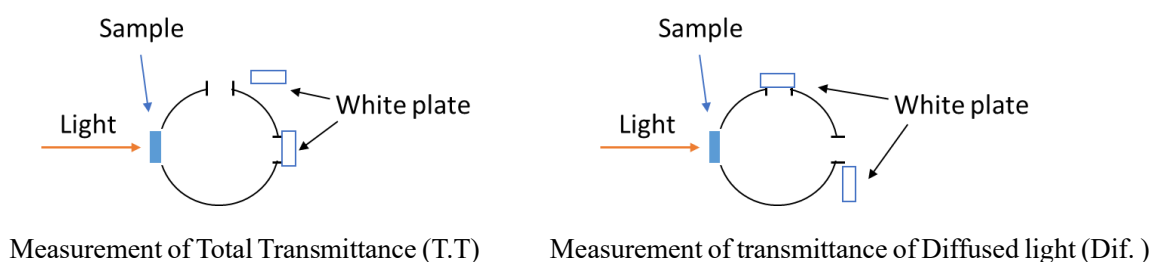


Figure 35. UV-vis spectra of polymers

4.2.2 Total transmittance and Haze

Total transmittance and Haze measurements were performed on NDH 7000 SP II Haze meter. The principle of instrument is shown in Figure 36. The haze meter can measure total transmittance (T.T) and transmittance of Diffused light (Dif.) by switching modes. The transmittance of diffused light is measured by directly measuring transmittance of parallel light, and then subtracting the parallel light from the total light to obtain diffused light. The percentage of light that deviates from the incident beam by greater than 2.5 degrees on average is defined as haze, and it can be calculated by the following formula as shown in Figure 36. The samples are prepared by the same method in 3.4. As shown in Table 11, the total transmittance of all polymer salts was above 90%, successfully excluding the influence of scattering light and proving that these polymers are colorless and transparent.



$$Haze = \frac{\text{transmittance of diffused light}}{\text{total transmittance}} \times 100 (\%)$$

Figure 36. The principle of haze meter and calculation of *Haze*

Table 11. Total transmittance and Haze of polymers

	T.T	Haze	P.T ^a	Dif.
Air ref.	100	0.00	100.	0.00
Glass ref.	91.1	0.19	90.9	0.17
PFA	91.6	0.34	91.3	0.31
PFA-Li	90.8	0.92	90.0	0.84
PFA-Na	90.4	19.6	72.7	17.7
PFA-K	90.9	0.59	90.3	0.54

^a Parallel light transmittance

CHAPTER 5. SUMMARY AND PROSPECTS

This thesis focused on colorless, transparent heat-resistant polymer materials. For conventional heat-resistant polymers, such as polyimide, which usually have darker color due to aromatic ring structure. They are difficult to use in electro and optical applications. Substituted polymethylene is the polymer with substituents on all their main chain carbon atoms which is expected to have unique properties due to their rigid main chain structure. The concept of polymer design starting from poly(acrylic acid) (PAA) to poly(fumaric acid) (PFA) by reducing the methylene spacers in the repeating units. Based on PFA, I tried to neutralize with different metal hydroxides to obtain poly(carboxylate) and cross-link with diamine or diol to increase the inter-chain interactions to improve thermal properties.

As the result of syntheses, the salts of PFA and cross-linked PFA were synthesized and characterized successfully. Two strategies have been attempted for salts of PFA, C1 polymerization from ethyl diazoacetate and free radical polymerization from di-tert-butyl fumarate. Since low molecular weight, inefficient hydrolysis, and potential explosiveness of diazo compounds in a large scale, C1 polymerization is not feasible for this study. There are also two strategies have been attempted for cross-linked polymers, esterification from acyl chloride and amidation by condensation agent. The cross-linking by condensation agent is controlled and can be used for synthesis of gels. However, a common problem with both methods is that it is difficult to purify the cross-linked polymers, resulting in their thermal properties are affected. Besides, the color left by the condensation agent is difficult to remove.

As for the characterization of polymers. Thermal properties, including T_d and T_g , are performed by Thermal Gravimetric (TG) analysis and Differential Scanning Calorimetry (DSC). Transmittance are measured by UV-vis spectrometer and Haze meter. Among them, sodium salt of PFA shows excellent thermal stability as well as light transmittance. And its heat-resistance and solubility can be adjusted by different degrees of neutralization. Although these polymers do not have T_g , it can be considered that the mechanical properties of materials do not change significantly up to the thermal decomposition temperature. It is acceptable as a heat-resistant material.

This category of polymers with a rigid main chain structure can be developed for additional applications through other modifications in the future. For instance, introducing functional groups to give the polymer liquid crystal, light-emitting, and temperature-responsive properties. For the aggregation morphology of PFA-Na, it was not fully explored in this study. In the future, it can be further investigated by TEM, radiography, and other material analysis.

ACKNOWLEDGMENTS

This thesis is based on the study carried out in the research group of Associate Professor Masanobu Naito and Lecturer Kazuaki Kato at Department of Advanced Materials Science, Graduate School of Frontier Sciences, The University of Tokyo, and Data-driven Polymer Design group at National Institute for Materials Science (NIMS) from 2020 to 2022. Much appreciation goes to people who have been helping and supporting me during these two years.

First of all, I would like to thank Prof. Masanobu Naito for giving many opportunities and kind guidance throughout my life and research. With his knowledge and experience, he was always able to provide constructive advice when my research was bottlenecked. Prof. Naito also helped me when I needed to use instruments that were not available in our group. I really appreciate his instructions.

I would like to thank Lecturer Kazuaki Kato for his help with the contacts to the University of Tokyo and for his guidance in polymer physics. I really appreciate his instructions and fixes for the format of my thesis. Discussing with Mr. Kato how to effectively use the resources provided by the university has benefited me a lot.

I would like to thank Researcher Y. Nakamura and Engineer T. Fujita of NIMS for their specific guidance on my experiments and for his valuable comments during the weekly research seminars. They helped me a lot to set up the experiments of organic synthesis. I really appreciate their instructions.

I would like to thank Prof. Kimiyoshi Naito for providing me with the thermogravimetric analysis instrument and Researcher Takanobu Hiroto for his help in using the instruments and analyzing the results of my XRD experiments.

I would like to thank all the members of Data-driven Polymer Design group, Mrs. Hanamura and Mrs. Yamamoto who helped me a lot by experimenting in the same lab as me, Mr. Matsuoka, a second-year master's student at Tsukuba University, and Kawai, Ryu, the graduates of the University of Tokyo, with whom I traveled, had dinners, and experienced Japanese culture that enriched my study abroad life. Thank you very much.

Finally, I must thank my family for their monetary and mental support.

July 2022
Wenhao Zhang

REFERENCES

1. Mehdipour-Ataei, S. & Tabatabaei-Yazdi, Z. *Heat Resistant Polymers. Encyclopedia of Polymer Science and Technology* (2015). doi:10.1002/0471440264.pst636.
2. Farbey, J., Sharpe, R. J. & Atrill, S. Scope of Review. *Law Habeas Corpus* 18–64 (2011) doi:10.1093/acprof:oso/9780199248247.003.0002.
3. Jin-gang Liu, Hong-jiang Ni, Zhen-he Wang, S. Y. and W. Z. Colorless and Transparent high – Temperature-Resistant Polymer Optical Films – Current Status and Potential Applications in Optoelectronic Fabrications. *Intech* 13 (2012).
4. Grulke, J. B. E. H. I. E. A. *Polymer handbook*. (2005).
5. Douglas, P., Andrews, G., Jones, D. & Walker, G. Analysis of in vitro drug dissolution from PCL melt extrusion. *Chem. Eng. J.* **164**, 359–370 (2010).
6. Artois, F. Influence of the melt temperature on the Thermoplastics Crystallization Process. **450**, 445–450 (1990).
7. Terao, Y., Sugihara, S., Satoh, K. & Kamigaito, M. 1:3 ABAA sequence-regulated substituted polymethylenes via alternating radical copolymerization of methyl cinnamate and maleic anhydride followed by post-polymerization reactions. *Eur. Polym. J.* **120**, 109225 (2019).
8. Otsu, T., Yasuhara, T., Shiraishi, K. & Mori, S. Radical high polymerization of di-tert-butyl fumarate and novel synthesis of high molecular weight poly(fumaric acid) from its polymer. *Polym. Bull.* **12**, 449–456 (1984).
9. Otsu, T. & Shiraishi, K. Monomer-isomerization radical polymerization of di-tert-butyl maleate to high-molecular weight poly(di-tert-butyl fumarate). **18**, 1795–1796.
10. Otsu, T., Yasuhara, T. & Matsumoto, A. Synthesis, Characterization, and Application of Poly (Substituted Methylene)S. *J. Macromol. Sci. Part A - Chem.* **25**, 537–554 (1988).
11. Otsu, T., Yoshioka, M. & Sunagawa, T. Radical polymerization of isopropyl tert-butyl fumarate and maleate, and characterization of the resulting polymers. **30**, 1347–1354.
12. Matsumoto, A. & Otsu, T. Synthesis and Radical Polymerization of Adamantyl-Containing Maleic and Fumaric Esters Leading to Formation of Thermally Stable Poly(substituted methylene)s with a Rigid Chain Structure. **20**, 1361–1364.
13. Otsu, T., Minai, H., Toyoda, N. & Yasuhara, T. Radical high polymerization of dialkyl fumarates with bulky substituents leading to less-flexible rod-like polymers. **12**, 133–142.
14. Otsu, T. & Toyoda, N. High molecular weight poly(methyl alkyl fumarates): radical high polymerization of methyl alkyl fumarates and monomer-isomerization radical polymerization of methyl alkyl maleates. **11**, 453–458.
15. Otsu, T., Yoshioka, M., Matsumoto, A. & Shiraishi, K. Synthesis of high molecular weight poly(dialkyl fumarate)s bearing n-alkyl side chains from poly(di-tert-butyl fumarate) via olefin elimination and reesterification in a one-pot. **26**, 159–164.
16. Otsu, T., Yasuhara, T., Shiraishi, K. & Mori, S. Radical high polymerization of di-tert-butyl fumarate

- and novel synthesis of high molecular weight poly(fumaric acid) from its polymer. **12**,
17. Jellema, E., Budzelaar, P. H. M., Reek, J. N. H. & de Bruin, B. Rh-Mediated Polymerization of Carbenes: Mechanism and Stereoregulation. **129**, 11631–11641.
 18. Ihara, E., Itoh, T. & Shimomoto, H. Polymerization of Alkyl Diazoacetates Initiated with Pd Complexes. **349**, 57–64.
 19. Ihara, E. *et al.* Pd-mediated polymerization of diazoacetates with aromatic ester group: Synthesis and photophysical property of poly(1-pyrenylmethoxycarbonylmethylene). **51**, 1020–1023.
 20. Ihara, E., Takahashi, H., Akazawa, M., Itoh, T. & Inoue, K. Polymerization of Various Alkyl Diazoacetates Initiated with (N)-Heterocyclic Carbene)Pd/Borate Systems. **44**, 3287–3292.
 21. Shimomoto, H., Asano, H., Itoh, T. & Ihara, E. Pd-initiated controlled polymerization of diazoacetates with a bulky substituent: synthesis of well-defined homopolymers and block copolymers with narrow molecular weight distribution from cyclophosphazene-containing diazoacetates. **6**, 4709–4714.
 22. Cahoon, C. R. & Bielawski, C. W. Metal-promoted C1 polymerizations. **374**, 261–278.
 23. Franssen, N. M. G., Reek, J. N. H. & Bruin, B. de. Pd-mediated carbene polymerisation: activity of palladium(II) versus low-valent palladium. **2**, 422–431.
 24. Shimomoto, H. *et al.* Polymerization of alkyl diazoacetates initiated by the amidinate/Pd system: efficient synthesis of high molecular weight poly(alkoxycarbonylmethylene)s with moderate stereoregularity. **8**, 4030–4037.
 25. Zhukhovitskiy, A. V *et al.* A Dinuclear Mechanism Implicated in Controlled Carbene Polymerization. **141**, 6473–6478.
 26. Jellema, E. *et al.* Rhodium-Mediated Stereospecific Carbene Polymerization: From Homopolymers to Random and Block Copolymers. **43**, 8892–8903.
 27. Jellema, E., Jongerius, A. L., Reek, J. N. H. & de Bruin, B. C1 polymerisation and related C–C bond forming ‘carbeneinsertion’ reactions. **39**, 1706–1723.
 28. Shimomoto, H., Kudo, T., Tsunematsu, S., Itoh, T. & Ihara, E. Fluorinated Poly(substituted methylene)s Prepared by Pd-Initiated Polymerization of Fluorine-Containing Alkyl and Phenyl Diazoacetates: Their Unique Solubility and Postpolymerization Modification. **51**, 328–335.
 29. Ihara, E. & Shimomoto, H. Polymerization of diazoacetates: New synthetic strategy for C-C main chain polymers. **174**, 234–258.
 30. Matsumoto, A. & Otsu, T. The Effect of Bulky Ester Alkyl Substituents on Rate Constants of Radical Polymerization of Dialkyl Fumarates. *Proc. Japan Acad. Ser. B* **70**, 43–47 (1994).
 31. Tsuji, N., Suzuki, Y. & Matsumoto, A. Adamantane-containing poly(dialkyl fumarate)s with rigid chain structures. *Polym. J.* **51**, 1147–1161 (2019).
 32. Kantor, S. W. & Osthoff, R. C. High Molecular Weight Polymethylene. *J. Am. Chem. Soc.* **75**, 931–932 (1953).
 33. Kato, F. *et al.* Self-Assembly of Hierarchical Structures Using Cyclotriphosphazene-Containing Poly(substituted methylene) Block Copolymers. **7**, 37–41.
 34. Kawaguchi, S., Toui, S., Onodera, M., Ito, K. & Minakata, A. Phase Separation Behavior in Neutralized

- Poly(maleic acid) Aqueous Solutions. *Macromolecules* **26**, 3081–3085 (1993).
35. El-Faham, A., Funosas, R. S., Prohens, R. & Albericio, F. COMU: A safer and more effective replacement for benzotriazole-based uronium coupling reagents. *Chem. - A Eur. J.* **15**, 9404–9416 (2009).
 36. Suzuki, Y., Tsujimura, T., Funamoto, K. & Matsumoto, A. Relaxation behavior of random copolymers containing rigid fumarate and flexible acrylate segments by dynamic mechanical analysis. *Polym. J.* **51**, 1163–1172 (2019).
 37. Suzuki, Y. *et al.* Relaxation behavior of poly(diisopropyl fumarate) including no methylene spacer in the main chain. **196**, 122479.
 38. Suzuki, Y. *et al.* Characteristic Features of α and β Relaxations of Poly(diethyl fumarate) as the Poly(substituted methylene). *Macromol. Chem. Phys.* **222**, 1–9 (2021).
 39. Kitano, T., Kawaguchi, S., Ito, K. & Minakata, A. Dissociation Behavior of Poly(fumaric acid) and Poly(maleic acid). 1. Potentiometric Titration and Intrinsic Viscosity. *Macromolecules* **20**, 1598–1606 (1987).
 40. Kawaguchi, S., Kitano, T. & Ito, K. Dissociation Behavior of Poly(fumaric acid) and Poly(maleic acid). 3. Infrared and Ultraviolet Spectroscopy. *Macromolecules* **25**, 1294–1299 (1992).
 41. Kawaguchi, S., Kamata, M. & Ito, K. Infrared and ultraviolet spectroscopic studies on intramolecular hydrogen bonding of poly(itaconic acid). *Polym. J.* **24**, 1229–1238 (1992).